Reviewed Preprint
v1 • December 18, 2025
Not revised

Reviewed Preprint
v2 • April 10, 2026
Revised by authors

Structural mechanisms of pump assembly and drug transport in the AcrAB–TolC efflux system

Xiaofei Ge[1,2] ✉, **Zhiwei Gu**[1], **Jiawei Wang**[1] ✉

[1]State Key Laboratory of Membrane Biology, Beijing Frontier Research Center for Biological Structure, School of Life Sciences, Tsinghua University, Beijing, China • [2]Health and Wellness, City University of Macau, Macau, China

✉ **For correspondence:**
gxf16@tsinghua.org.cn
jwwang@tsinghua.edu.cn

Competing interests: No competing interests declared

Funding: See page 21

Reviewing editor: Lejla Zubcevic, University of Kansas Medical Center, United States

eLife Assessment

Ge et al here report a structural study of the native tripartite multidrug efflux pump complexes from Escherichia coli that identifies a novel accessory subunit, YbjP, the structure of the native TolC-YbjP-AcrABZ complex, as well as structures of the AcrB protein in L, T, and O conformations. The strength of the structural data is **compelling**, and the importance of the findings is potentially **fundamental**. In the revised manuscript, the authors have included additional analysis and made comparisons with pre-existing data which has helped place the data and its impact in the proper context.

https://doi.org/10.7554/eLife.109684.2.sa3

Abstract

Tripartite multidrug efflux pumps that span the cell envelope are essential for antibiotic resistance in Gram-negative bacteria. Here, we report cryo-EM structures of two endogenous efflux complexes from *Escherichia coli*: a TolC–YbjP subcomplex at 3.56 Å resolution and the complete TolC–YbjP–AcrABZ pump at 3.39 Å. Structural analysis reveals that YbjP, a previously uncharacterized lipoprotein, binds TolC in a 3:3 stoichiometry, bridging the TolC protomers at their equatorial domain. Clear density of the mature YbjP's N-terminal Cys19 indicates that YbjP is anchored to the outer membrane by an N-terminal lipid moiety. Notably, YbjP remains bound as TolC undergoes AcrA-induced opening, suggesting that this accessory protein accommodates the conformational change. The AcrB trimer simultaneously presents three distinct conformational states (L, T, O), capturing a complete transport cycle. These high-resolution structures provide insights into the architecture and mechanism of clinically relevant efflux machinery, identifying YbjP as a previously unrecognized structural component that contributes to TolC positioning and may assist in its membrane localization.

Introduction

Tripartite efflux pumps are essential for Gram-negative bacteria to expel a wide range of toxic compounds, including antibiotics, across their dual-membrane cell envelope[1–5]. Among these systems, the AcrAB–TolC complex of *Escherichia coli* is one of the most thoroughly studied[2,6]. It comprises the inner membrane RND (Resistance–Nodulation–Division) transporter AcrB, the periplasmic membrane fusion protein AcrA, and the outer membrane channel TolC[4,6–9]. AcrA, anchored to the inner membrane via N-terminal lipidation, bridges AcrB and TolC, mediating conformational signaling essential for TolC gating[10–12]. The assembling pathway of the tripartite pump involves the formation of an AcrA–AcrB subcomplex, followed by the recruitment of TolC to form the complete efflux apparatus[13]. In its isolated form, the periplasmic tip of TolC adopts a closed conformation, stabilized by interactions between the α-helices[14–16]. Structural studies have shown that TolC transitions from a closed to an open state in response to AcrAB assembly, a process crucial for efflux activation[13,17].

Despite significant progress in structurally characterizing the AcrAB–TolC system, fundamental questions remain regarding how TolC is positioned and retained in the outer membrane. Unlike homologous channels such as *Pseudomonas aeruginosa* OprM[18] and *E. coli* CusC[19], which possess covalently attached N-terminal lipids, TolC lacks a lipid anchor. This raises the possibility that *E. coli* may utilize accessory factors to localize and stabilize TolC during pump assembly. Furthermore, while prior studies using crystallography and cryo-EM have revealed low-to-medium resolution snapshots of the assembled pump[10–13,17,20], the limited resolution and conformational heterogeneity in those structures impeded accurate modeling of flexible regions and may have masked the presence of additional subunits.

Here, we address these knowledge gaps by determining two high-resolution cryo-EM structures of the TolC-based efflux machinery in *E. coli*. The first is a 3.56 Å structure of a TolC–YbjP subcomplex, and the second is a 3.39 Å structure of the fully assembled TolC–YbjP–AcrABZ pump. These structures reveal a previously uncharacterized outer membrane lipoprotein, YbjP, bound to TolC, and shed light on how TolC is secured and transitions to the open state. Together, these findings enhance our understanding of the architecture, assembly, and regulation of this clinically important efflux pump.

Results

Structure of a TolC–YbjP closed-state complex

Endogenous purification of *E. coli* membranes yielded a stable assembly containing the outer-membrane channel TolC (Figure S1A). The complex was purified directly from *E. coli* as a stoichiometric assembly, without the need for artificial fusion or crosslinking. Cryo-EM analysis resolved the complex at 3.56 Å resolution (Figures S1B-E, Supplementary Table S1). TolC forms a homotrimer composed of a β-barrel that spans the outer membrane and an elongated periplasmic α-helical domain (Figures 1A-D). The periplasmic α-helical domain comprises an α-helical barrel extended by two helix-turn-helix (HTH) motifs at its periplasmic extremity (TolC repeat 1: helices H3-H4; repeat 2: helices H7-H8). These structural elements converge at an equatorial domain (Figures 1C-D). The inward-bending HTH coiled-coils occlude the periplasmic tunnel, maintaining TolC in a closed conformation—consistent with previous crystal structures[10] (Figure 1C).

An unexpected density at the periplasmic face of TolC indicated the presence of an additional component (wheat in Figures 1A-B). An initial backbone trace, followed by a DALI search[21] tentatively matched Tai3, a periplasmic type IV immunity protein associated with the T6SS amidase effector Tae3 (PDB ID: 4HZ9)[22] from *Ralstonia pickettii.* However, discrepancies in side chain density and species origin indicated that the match was likely incorrect. Systematic screening of the AlphaFold Database[23] using CryoNet[24] identified *E. coli* YbjP (UniProt P75818) as the top candidate, with all side chains matching the experimental density (Figure S2). YbjP features a globular domain and a structured N-terminal loop stabilized by a Cys36-Cys144 disulfide bond (Figures 1E-F). The N-terminal loop of YbjP adopts an extended conformation parallel to the Helix 2 (residues 38-61) of TolC's α-helical barrel, forming substantial intermolecular interfaces. Buried surface area (BSA) analysis reveals 787 Å² of contact with the primary TolC protomer (green in Figure 1F), and 1037.4 Å² with the adjacent protomer (light green), suggesting asymmetric binding energetics. The N-terminal density extends to Cys19, which corresponds to the predicted signal peptide cleavage site, positioning the lipoprotein at the periplasmic face of the outer membrane.

UniProt predictions indicate that YbjP is dually lipidated via N-palmitoyl and S-diacylglycerol modifications, allowing its anchorage to the outer membrane. This represents an elegant evolutionary solution, as while many Gram-negative TolC homologs (*e.g.*, *P. aeruginosa* OprM[18], *E. coli* CusC[19], *et al.*) possess native lipid anchors (Figure S3), *E. coli* TolC instead recruits YbjP as a dedicated membrane-tethering partner. The YbjP globular domain nestles between adjacent TolC equational domains, forming a stable 3:3 complex (Figure 1B). The identification of YbjP, along with its defined membrane anchoring and structural compatibility with TolC, suggests a new class

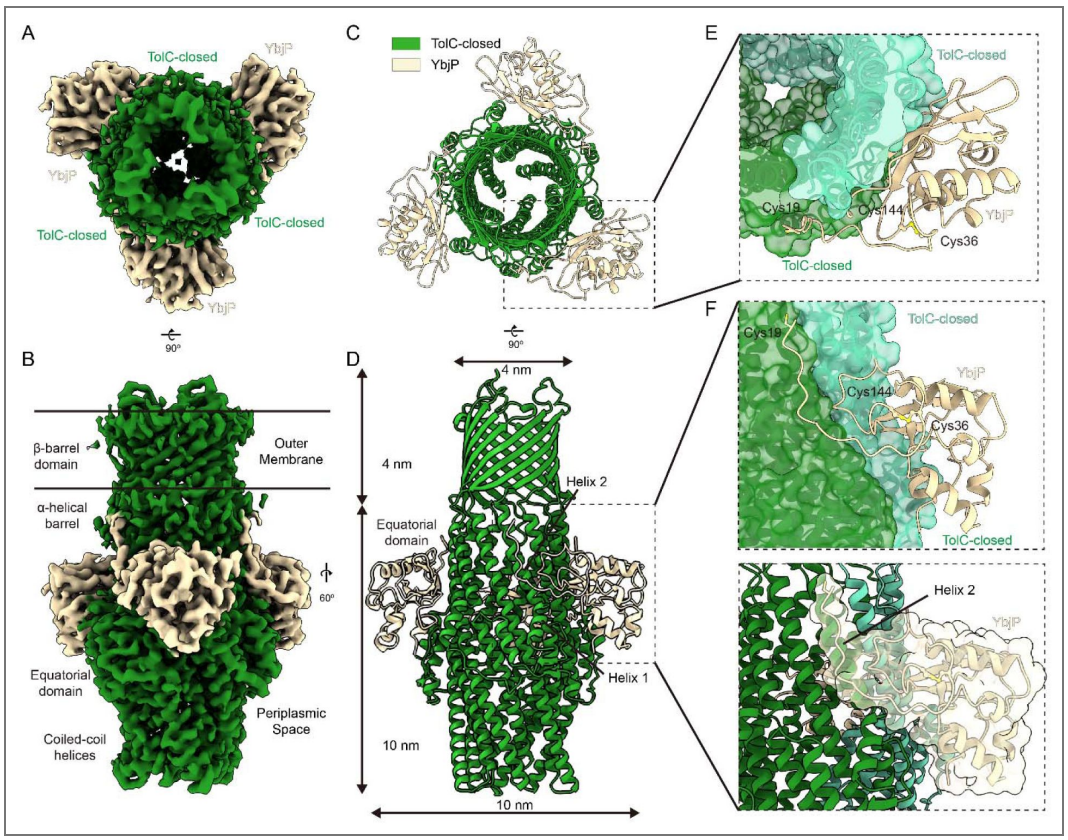

Figure 1. Structure of the TolC–YbjP complex (closed state).

(A,B) Cryo-EM density map of the endogenous TolC–YbjP complex at 3.56 Å resolution, shown in top and side view, spanning the outer membrane (OM) and periplasmic space. TolC forms a homotrimeric "channel-tunnel" ~14 nm long, with its 12-stranded β-barrel embedded in the OM and periplasmic coiled-coils sealed at the tip. YbjP (wheat) wraps around the equatorial domain of TolC, with continuous density linking YbjP's N-terminal Cys19 into the OM micelle region. **(C,D)** Top view (from the outer membrane) and side view of the TolC–YbjP cartoon model, showing three YbjP molecules arranged symmetrically around TolC's threefold axis. **(E,F)** Each YbjP straddles the interface between two TolC protomers, occupying a groove on the TolC surface. TolC is shown as surface and cartoon (each protomer in a different green color) and YbjP in wheat cartoon. YbjP's globular domain inserts between TolC protomers, while an N-terminal linker connects to the OM.

of outer membrane partners that may regulate the TolC-dependent pathways. Notably, the structure of TolC shows no conformational changes upon YbjP binding when compared to the free, closed form of TolC[10].

Structure of TolC–YbjP–AcrABZ complex

An improved 3.39 Å resolution structure of the endogenous AcrAB–TolC complex from *E. coli* was determined, revealing well-resolved density across the entire assembly (Figure S4, Supplementary Table S1). This structure allows for the accurate modeling of side-chain interactions throughout the tripartite channel, surpassing earlier models in completeness and resolution[17] (Figures S5-6). YbjP remains bound to TolC[25], suggesting that this lipoprotein is stably retained during pump assembly and functions as a molecular clamp that anchors TolC to the outer membrane during AcrA and AcrB engagement (Figures 2A-D).

The TolC–YbjP–AcrABZ complex adopts a funnel-like architecture spanning the cell envelope, consistent with prior models of tripartite pumps[17] (Figure 2B). TolC, tethered to YbjP, caps the outer-membrane end and docks onto a hexameric ring of AcrA adaptors in the periplasm, which in turn surrounds the AcrBZ trimer embedded in the inner membrane (Figures 2B, 2D). The full assembly is about 33 nm tall, comprising a 14 nm TolC channel, a 14 nm periplasmic portion of AcrAB, and a 5 nm transmembrane portion of AcrBZ, matching the distance between the two membranes (Figure 2B).

Cryo-EM density reveals six AcrA molecules positioned beneath each TolC trimer (Figure 2D), yielding a 3:6:3 stoichiometry for TolC:AcrA:AcrB. AcrA therefore forms an elongated hexamer that bridges TolC and AcrB. This tripartite architecture is stabilized by three distinct sets of interfaces: (i) contacts between the AcrB trimer and the basal regions of AcrA, (ii) extensive AcrA–AcrA lateral interactions within the hexameric ring, and (iii) tip-to-tip junctions formed between the upper AcrA α-helical hairpin and the periplasmic entrance of TolC (Figure 2D). While each AcrA protomer maintains the characteristic four-domain architecture—comprising the α-helical hairpin, lipoyl, β-barrel, and membrane-proximal domains—functional asymmetry is observed in their interactions (Figure 2E). The trimeric TolC, which contains six HTH motifs due to internal repeats (TolC repeat 1/2), engages the AcrA hexamer via quasi-equivalent binding: adjacent AcrA and AcrA* protomers interact differentially with the intra- and inter-protomer grooves of TolC, respectively (Figure 2F). The primary structural difference between AcrA and AcrA* lies in the configurations of their membrane-proximal (MP) domains (Figure 2E).

AcrB assembles as a homotrimer on the inner membrane, with each protomer comprising three distinct domains: a funnel/docking domain, a porter/periplasmic domain, and a transmembrane domain (Figure 2D). The funnel domain consists of two subdomains, DN and DC (denoting the N- and C-terminal subdomains) (Figure 2G). The porter domain is organized into four subdomains – PN1, PN2, PC1, and PC2 – named for the N- and C-terminal subdomains. When viewed from the periplasmic side, these subdomains are arranged in a clockwise orientation, with PN1 positioned closest to the central axis of the trimer. In the hexameric AcrA assembly, the lipoyl and β-barrel domains form two stacked concentric rings. While the lipoyl domains remain uninvolved in AcrB binding, the β-barrel domains specifically engage the funnel domain of AcrB. Strikingly, the membrane-proximal (MP) subdomains of AcrA exhibit asymmetric binding: AcrA–MP interacts with the DC and PC1 subdomains of AcrB, whereas AcrA*–MP contacts PN1 and DN via an extended loop, respectively (Figures 2G-H). This differential engagement of MP subdomains establishes the structural basis for the observed structural divergence between AcrA and AcrA* (Figure 2E).

Our density maps clearly resolve the small transmembrane protein AcrZ (49 amino acids) bound to each AcrB protomer (Figures 2B, 2D). AcrZ adopts a helical structure that is embedded within a hydrophobic groove formed by the transmembrane helices of AcrB at the predicted interaction site, forming an AcrB AcrZ complex. Although AcrZ is not essential for pump assembly, its consistent presence in endogenously purified complexes and its role in stabilizing otherwise flexible regions—particularly the transmembrane helices—suggest that AcrZ may serve an allosteric role in modulating conformational dynamics for specific substrates[26]. Collectively, these

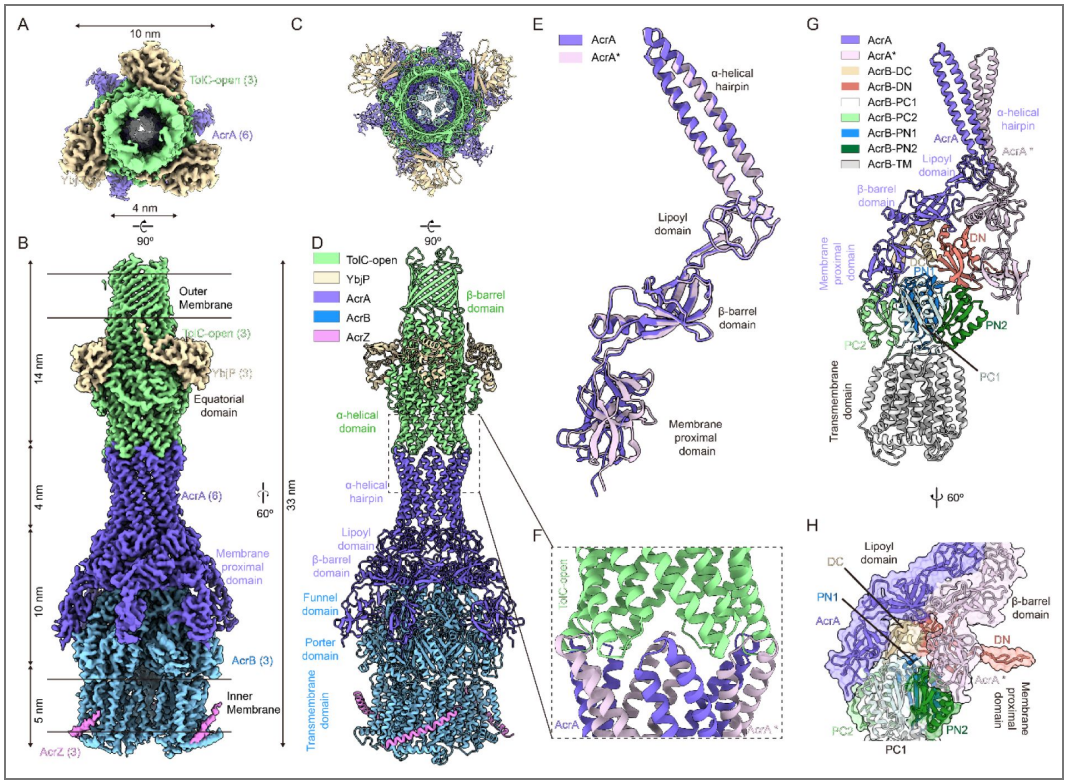

Figure 2. Architecture of the fully assembled TolC–YbjP–AcrABZ efflux pump.

(A,B) Top and side view of the cryo-EM density map (3.39 Å) of the endogenous TolC–YbjP–AcrABZ complex, with the inner membrane (IM) and outer membrane (OM) boundaries indicated (black bars). The map reveals the complete pump spanning 33 nm. Densities for TolC (green) are supposed to be in the OM region, AcrB (blue) in the IM region as a trimer, and six AcrA protomers (purple) forming an elongated barrel bridging TolC and AcrB. Three AcrZ protomers (pink) are seen at the periphery of the AcrB trimer in the IM region. **(C,D)** Cartoon models of TolC–YbjP–AcrABZ in top view and side view. Three AcrB protomers (blue) form a trimeric base, surrounded by six AcrA molecules (purple) and three AcrZ helices (pink). Each AcrB protomer consists of funnel, porter, and transmembrane domains. **(E)** Structural alignment of the two AcrA conformations (AcrA and AcrA*) reveals differences in the orientation of membrane proximal domain. **(F)** Zoomed-in view of the TolC–AcrA interface, show the tight interaction between TolC's periplasmic helix-turn-helix motifs and AcrA's α-helical hairpin domain. **(G,H)** Close-up views of the interface between AcrA (purple), AcrA* (light purple), and AcrB. Panel (G) shows the frontal cartoon representation; panel (H) displays a 60° rotated view, highlighting the intimate packing of AcrA with AcrB.

interactions illustrate the sophisticated assembly mechanism of the pump: AcrZ reinforces AcrB's transmembrane domain, AcrB's funnel and porter domains anchor AcrA, and AcrA's α-helical hairpins engage TolC. Notably, the holocomplex remained intact throughout purification, indicating a high-affinity assembly between components, consistent with prior *in vitro* reconstitution studies[25].

Structural rearrangements underlying TolC's closed-to-open transition

A comparative structural analysis of TolC in its closed and open states reveals a striking iris-like dilation mechanism at the periplasmic entrance that facilitates transition to the fully open conformation (Figures 3A-B)[27]. Throughout this conformational transition, the transmembrane β-barrel and α-helical barrel domains maintain remarkable structural rigidity, whereas the coiled-coil helices undergo dramatic rearrangement. These helices pivot around the equatorial domain, undergoing a 27° rigid-body superhelical rotation (Figure 3C), which constitutes a major structural rearrangement. In the closed state, a complex network of interprotomer hydrogen bonds stabilizes the structure by constricting the pore to its narrowest point at Asp396 (Figures 3D, 3F)[28,29]. Upon disruption of this network in the open state, the pore expands significantly, reaching a diameter of approximately 2 nm (Figures 3E-F). Notably, YbjP remains stably association with TolC in both conformational states – the closed resting state and the open activated state (Figure 3C). This persistent interaction suggests that YbjP serves as a structural scaffold: anchoring TolC in the outer membrane, accommodating conformational changes during activation, and functionally compensating for TolC's lack of intrinsic lipidation (Figure S3). These findings not only support existing models of allosteric pump activation[12,17,20,27,30], but also suggest how *E. coli* might utilize YbjP to fulfill the membrane-anchoring role typically provided by intrinsic lipid modifications in other bacterial TolC homologs, such as OprM and CusC[31,32].

Mechanism of substrate transport in the AcrB module

The AcrAB–TolC efflux system actively transports substrates against their concentration gradient, moving them from regions of low to high concentration. This energetically unfavorable process is driven by proton motive force (PMF), with the AcrB trimer harnessing the electrochemical potential of protons to power substrate translocation[33]. Structural and functional studies support an asymmetric rotary mechanism[32], wherein each AcrB protomer sequentially transitions through three conformational states: L (loose), T (tight), and O (open)[20,34]. This concerted conformational rotation – analogous to the functional cycling of F_1F_0 ATP synthase during ATP synthesis – enables continuous vectorial transport through the pump complex[35].

Our high-resolution cryo-EM structure of the endogenous TolC–YbjP–AcrABZ complex captures the AcrB trimer in three distinct conformational states (L, T, O), providing key mechanistic insights (Figures 4A, S7). The detailed conformational changes associated with this functional rotation mechanism are distinctly different from those observed in isolated AcrB structures[36], even those determined in the native membrane environment[37] (Figure S8).

The transmembrane domain of AcrB consists of N- and C-terminal transmembrane repeats (N-TMR and C-TMR), encompassing TM1-TM6 and TM7-T12, respectively (Figure 4B). Key proton relay residues – D407 and D408 on TM4, and K940 and R971 on TM10 – are located within these domains. While the transmembrane domain remains largely conserved between the L and T states (Figure 4B, upper panel) – maintaining salt bridges between Lys940 (TM10) and Asp407/Asp408 (TM4), the T→O transition entails a coordinated rotation of TM2, TM4, TM5, and TM6, disrupting these interactions (Figure 4B, lower panel).

In the L state, the PC1 and PC2 subdomains form a cleft that constitutes part of the access pocket (AP). Substrate entry occurs between PC1 and PC2 in the L state (Figure 4C, left panel). A conformational change to the T state is initiated by a random-coil-to-helix transition in the upper part of TM8, coupled with an 8 Å shift of PC2 toward PC1 (Figure 4D, middle panel and Figure S7). This displaces the switch loop that separates the AP from the deep binding pocket (DBP),

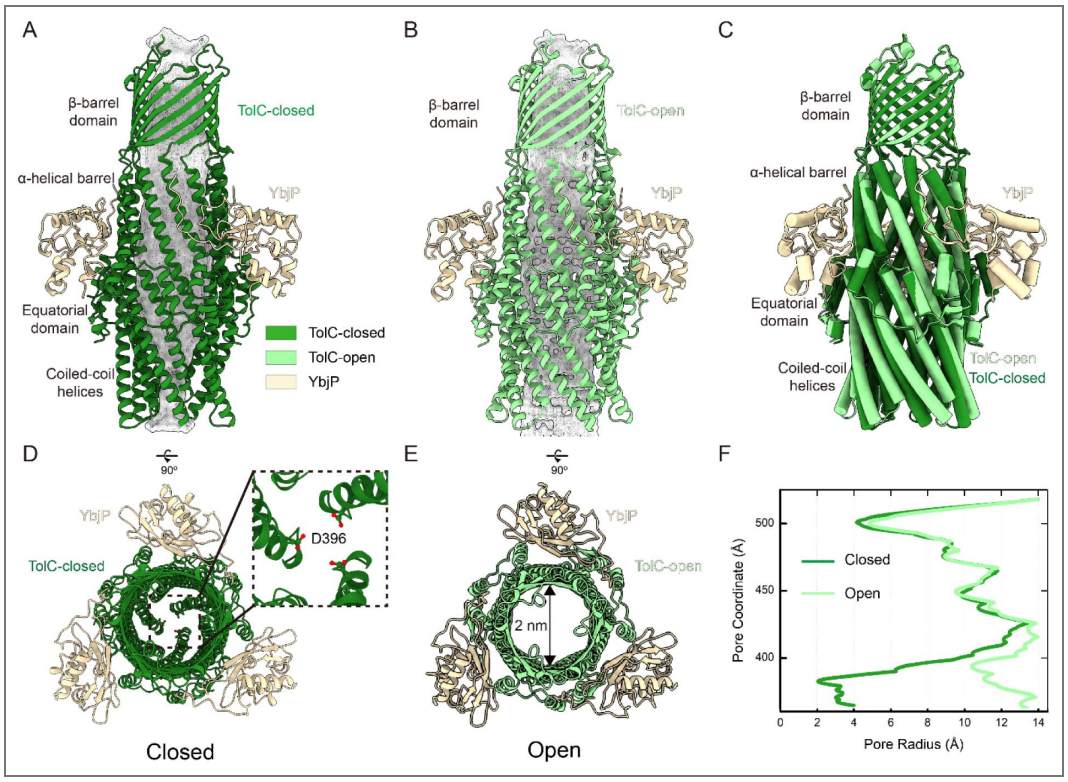

Figure 3. Conformational changes upon pump assembly: closed to open TolC transition.

(A) Side view of TolC–YbjP complex. TolC is closed by coiled-coil helices. **(B)** Side view of TolC–YbjP part in TolC–YbjP–AcrABZ complex. TolC is in open state. **(C)** Comparison of TolC in the TolC–YbjP complex (closed state, forest green) and in the TolC–YbjP–AcrABZ pump (open state, pale green). Upon assembly with AcrABZ, these contacts are disrupted and the TolC helices tilt outward, enlarging the aperture. The OM β-barrel domain remains static. YbjP positions are consistent in two structures. **(D,E)** Top views of TolC–YbjP in closed *vs.* open states. In the closed conformation, the coiled-coil helices bundle tightly, leaving a ~4 Å diameter sealed pore. In the open state (pale green), the helices are splayed apart, creating a ~20 Å diameter open channel. **(F)** Quantitative comparison of pore radii in closed and open TolC, as computed using HOLE software[53].

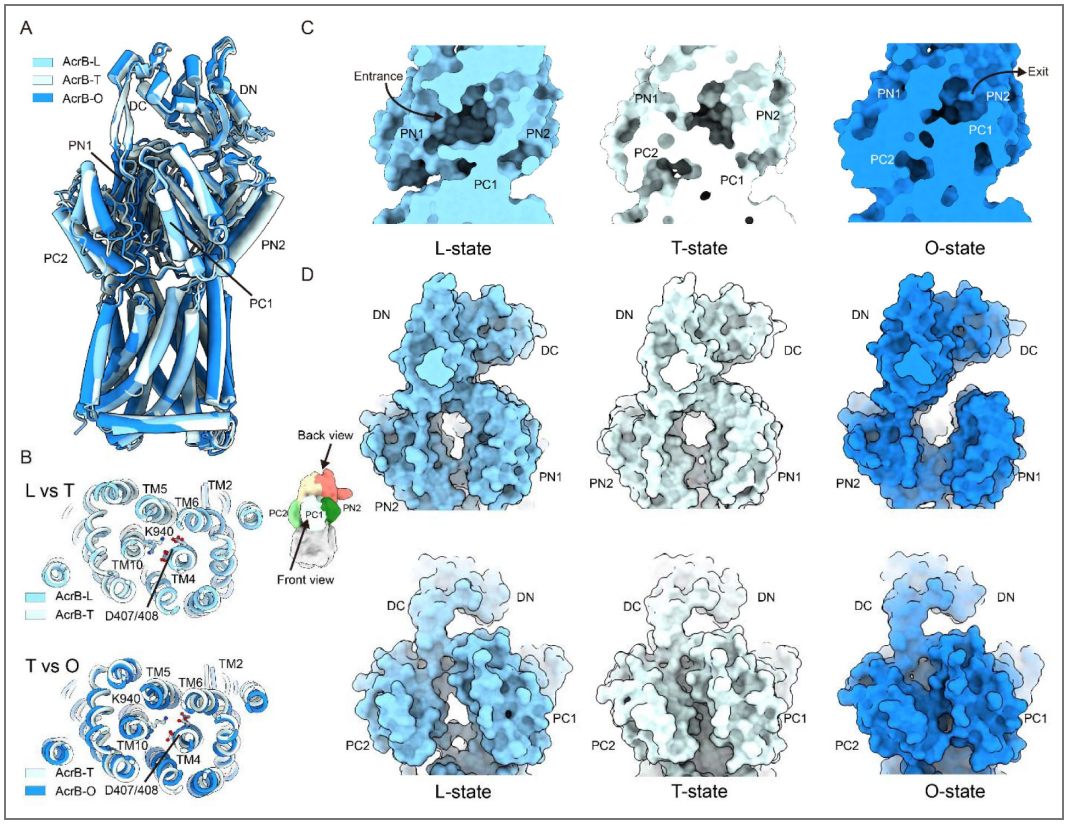

Figure 4. Conformational cycling of AcrB monomers within the functional trimer.

(A) Structural superimposition of the three AcrB protomers (L, T, O states) showing their sequential conformational transitions during the transport cycle. **(B)** Conformational changes in the transmembrane domain associated with proton translocation. **(C)** Substrate-binding pocket architecture in a single protomer, highlighting subdomains involved in drug recognition. **(D)** Large-scale structural rearrangements in the porter domain that facilitate substrate translocation.

facilitating drug transfer from the AP to the high-affinity DBP (Figure 4C, middle panel). Remarkably, PC1 remains static and in contact with AcrA throughout the cycle (Figure S7). Transition to the O state is triggered by the protonation of D407 and/or D408. This causes an inward-facing movement of the N-TMR and C-TMR, bringing PC2 even closer to PC1 (Figure 4D, right panel). Concurrently, PN1 and PN2 subdomains move closer together on the transmembrane side, closing the DBP (Figure 4D, right panel). These collective movements open a continuous tunnel that extends to the funnel domain, enabling substrate extrusion (Figure 4C, right panel). The release of protons into the cytoplasm, down their electrochemical gradient, subsequently restores the charge on D407 and/or D408, resetting the transmembrane domain to its engaged state. This rotary mechanism, reminiscent of F_1F_0 ATP synthase, is completed when the pump resets to the L state, initiating a new catalytic cycle.

Discussion

Based on our structural data, we propose a model for the assembly and function of the AcrAB–TolC multidrug efflux pump, emphasizing the anchoring and orienting role of YbjP. As shown in Figure 5, the assembly begins with TolC priming. In the absence of AcrAB, TolC is embedded in the outer membrane in a closed conformation, stabilized by its interaction with YbjP. The lipid moiety of YbjP inserts into the inner leaflet of the outer membrane, providing structural compensation for TolC's lack of intrinsic lipid anchoring (Figure S3). Additionally, the periplasmic side of TolC may transiently interact with the peptidoglycan layer, helping to position it within the periplasmic space. This anchoring likely ensures optimal orientation of TolC's periplasmic end for interaction with incoming AcrA.

Upon synthesis and membrane insertion, AcrB (complexed with AcrZ) and AcrA form an inner membrane–periplasmic subcomplex[38,39]. A conserved cysteine residue in AcrA, located near the inner membrane, may aid in anchoring or stabilizing the complex. The complete tripartite pump likely assembles via stochastic encounters between the endogenous AcrABZ subcomplex and the TolC–YbjP complex in the periplasm. Stabilization likely occurs through tip-to-tip interactions between the hairpin domains of AcrA and TolC[40]. YbjP may facilitate this docking by stabilizing TolC in a fixed, properly oriented conformation at the outer membrane, thereby increasing its local availability to the endogenous AcrABZ and lowering the energy barrier for tripartite pump assembly, which is supported by the comparative structural analysis of TolC homologs (Figure S3). In this context, YbjP may act as a structural placeholder that guides AcrA toward the TolC entrance without directly modulating TolC's gating or AcrABZ's conformational dynamics. YbjP's consistent presence in our cryo-EM reconstructions of endogenous complexes and its predicted lipoprotein features together suggest a specialized anchoring role for TolC (Figure S3). Based on our structural observations and UniProt annotations, we propose that YbjP contributes to TolC stabilization in the outer membrane and facilitates its spatial orientation for efficient pump assembly.

Once assembled, the AcrABZ–TolC complex becomes active for drug efflux, allowing substrates such as antibiotics and dyes to enter AcrB from the periplasm and be expelled through TolC[41,42]. At the core of this process is the conserved D407–D408 proton relay pair in AcrB's transmembrane domain, which functions as both the proton-binding site and the mechanochemical coupling hub[43,44]. Protonation of these residues initiates conformational changes that propagate from the transmembrane domain to the porter domain via an allosteric mechanism, which is refined in the context of the intact endogenous pump complex.

The AcrB trimer operates via an asymmetric rotary cycle[20,34], with each protomer sequentially transitioning through three distinct conformational states (L → T → O) to drive peristaltic drug transport. This concerted conformational rotation – bearing striking similarity to the catalytic cycle of F1F0 ATP synthase – enables continuous, vectorial substrate transport against concentration gradients powered by proton translocation, and our data reveal subtle yet functionally relevant conformational differences of this cycle in the intact endogenous pump compared to isolated AcrB (Figure S8).

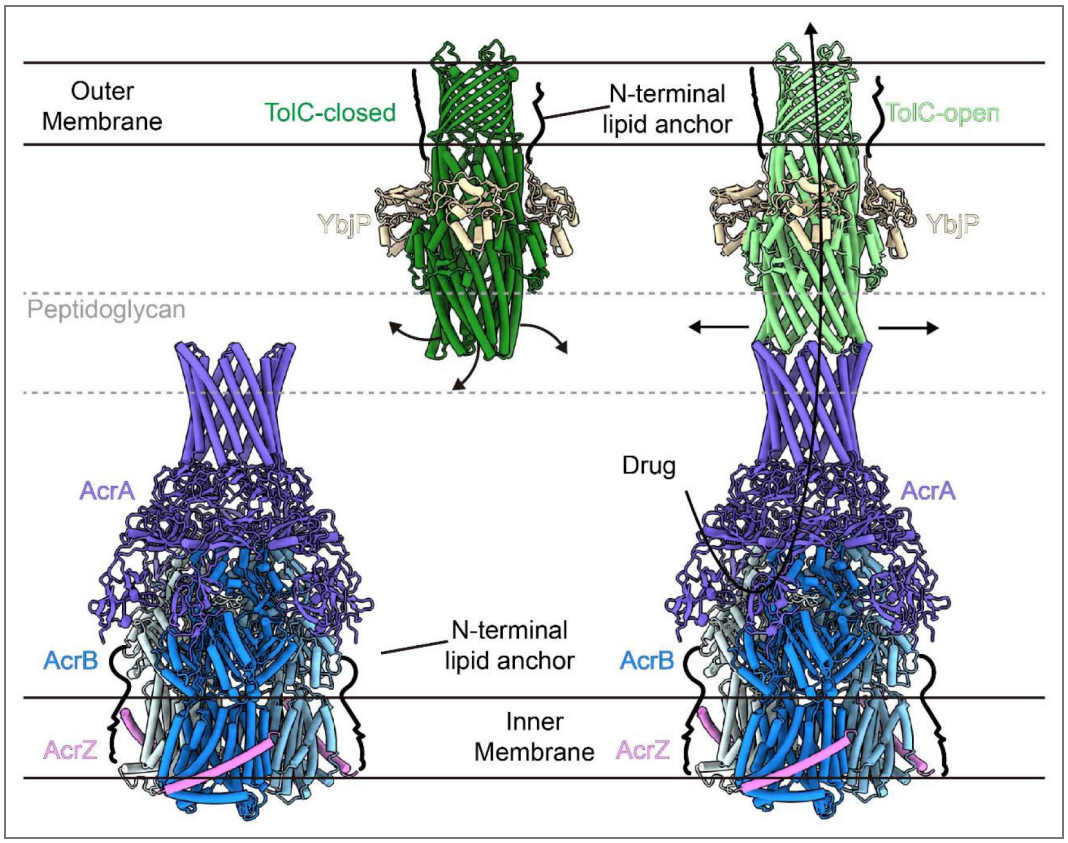

Figure 5. Proposed model of pump assembly and membrane anchoring.

Schematic illustration of the TolC–YbjP–AcrABZ efflux pump within the Gram-negative cell membrane. YbjP is hypothesized to associate with the outer membrane via its N-terminal Cys19, which may undergo lipidation *in vivo*. YbjP lies just beneath the outer membrane and above the peptidoglycan layer, according to prior electron tomography studies[13]. In the absence of AcrABZ, TolC adopts a closed state stabilized by inward-pointing periplasmic helices. AcrA, also likely lipid-anchored at its N-terminus, stabilizes the AcrBZ trimer near inner membrane. Upon engagement with AcrA's α-helical hairpin domain, TolC helices rotate outward in a left-handed (counterclockwise) manner to open the channel, and enables small-molecule substrates to be exported through the fully assembled complex.

In conclusion, we identify YbjP as a previously unrecognized lipoprotein associated with the AcrAB–TolC efflux system. Although its precise function requires further validation, YbjP's structural positioning in the endogenous complexes suggests a specialized role in anchoring TolC at the outer membrane and promoting tripartite pump assembly (Figure S3), a process critical for bacterial multidrug resistance to antibiotics and toxic compounds. Notably, our high-resolution cryo-EM structures capture all three conformational states of the AcrB trimer (L, T, O) within the context of the fully assembled, endogenous TolC–YbjP–AcrABZ complex for the first time. While these states have been observed in isolated AcrB previously, our data reveal subtle yet functionally relevant conformational differences that arise in the intact endogenous pump (Figure S8), which are shaped by the native constraints of AcrA and AcrZ binding. This study exemplifies how high-resolution cryo-EM, in combination with integrative modeling, can reveal previously uncharacterized protein factors and enhance our understanding of complex membrane-spanning systems in bacteria.

Method details

Cell preparation and membrane protein extraction

E. coli C600 cells were cultured to mid-log phase and then infected with a high-titer λ phage to increase cellular stress. Cells were harvested by centrifugation and resuspended in buffer containing 25 mM Tris-HCl and 150 mM NaCl (pH 8.0). Lysozyme was added to a final concentration of 10 mg/mL, followed by incubation at 37 °C for 2 hours to facilitate cell lysis. Following removal of cell debris by centrifugation at 24,793 × g for 20 min, membrane proteins were extracted from the supernatant using 2% n-dodecyl-β-D-maltoside (DDM). The membrane fraction was subsequently subjected to size-exclusion chromatography using a SR6 Increase column. Fractions around 12 mL, which were enriched for target proteins, were collected, diluted, and used for negative staining. Transmission electron microscopy revealed the presence of target particles.

Cryo-EM grid preparation

The sample was concentrated to 0.7 mg/mL. A volume of 4 μL was applied to a glow-discharged Au Quantifoil R1.2/1.3 300 mesh grid (glow discharge: medium setting, 30 s). To enhance the concentration of protein on the grid, sample loading was repeated ten times: after each loading, excess solution was gently removed using a pipette tip, and a fresh 4 μL aliquot was applied. The grid was then plunge-frozen in liquid ethane pre-cooled with liquid nitrogen using a Vitrobot Mark IV (Thermo Fisher Scientific). Blotting was performed for 3.5 s after a 30 s wait time, under 100% humidity at 8 °C.

Cryo-EM data collection

A total of 3452 movies were acquired using a 300 kV Titan Krios transmission electron microscope (Thermo Fisher Scientific) equipped with a Gatan K3 Summit direct electron detector. The calibrated pixel size was 0.675 Å. Each movie was recorded with a total electron dose of ~50 $e^{-}/Å^{2}$, and defocus values ranged from -1.2 to -1.8 μm. Data collection was automated using the AutoEMation software[45].

Image processing

Motion correction and contrast transfer function (CTF) estimation were carried out in CryoSPARC[46]. Poor-quality micrographs were manually excluded. 43,200 particles corresponding to TolC were identified during 2D classification. Ab-initio reconstruction and NU-refinement applied with C3 symmetry generated a reference model for further picking. Template picking, *ab-initio* reconstruction in C1 symmetry, and NU-refinement in C3 symmetry followed. The resulting map at 4.17 Å resolution was further improved to 3.56 Å after reference-based motion correction (RBMC), CTF refinement, and NU-refinement.

From the same dataset, TolC–AcrABZ particle selection was performed using blob picking, followed by particle extraction and several rounds of 2D classification, which yielded 19,396 high-quality particles. These were used for ab-initio reconstruction and non-uniform (NU) refinement to generate an initial 3D model, which was subsequently used for template picking. After template picking and further 2D classification, a total of 35,092 particles were selected. Final refinement steps—including NU-refinement, RBMC, and local CTF refinement – resulted in a 3D map at 3.23 Å resolution. Since the AcrB subunit exhibits intrinsic structural asymmetry, C3 symmetry was initially relaxed through symmetry expansion combined with 3D classification without rotational/translational alignment. One predominant class was selected after deduplication of symmetry-expanded particles. Local refinement in C1 symmetry better resolved the asymmetric AcrB region. A subsequent masked 3D classification revealed a particle subset containing distinct extra densities, which underwent local refinement with re-applied C3 symmetry to enhance resolution of symmetric structural components.

Protein model building and structure refinement

The atomic models of TolC, AcrA, AcrB, AcrZ were rigid-body fitted into their corresponding cryo-EM maps using UCSF Chimera[47]. To identify the extra densities observed in both EM maps, a backbone model was manually traced. Protein identity was assessed using the "Protein Searching without Sequence" function in CryoNet[24]. YbjP (P75818) was ranked highest among *E. coli* proteins in the AlphaFold Database (AFDB, strain 4364). Side-chain densities in the final EM maps were manually compared to the predicted model, allowing confirmation of YbjP as the protein corresponding to the extra density. Subsequent manual adjustments to the models were performed using COOT[48]. The refinement of the protein structures was conducted using either PHENIX[49] or Refmac5[50]. Statistical details regarding the 3D reconstruction and model refinement processes are provided in Supplementary Table S1. Visual representations of the structures were generated using PyMol[51] or UCSF ChimeraX[52].

Supplementary information

Supplementary Figures

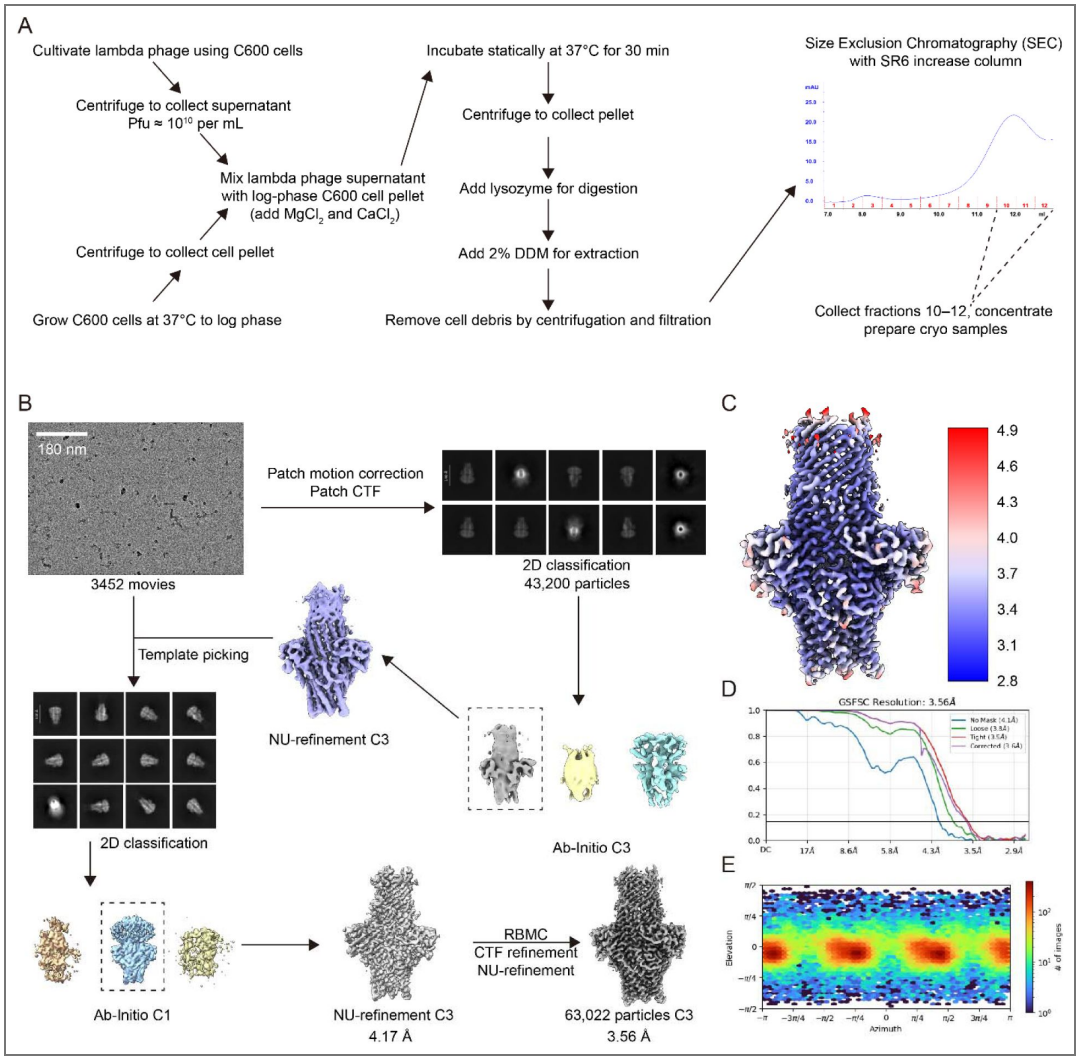

Figure S1. Cryo-EM processing workflow for TolC-YbjP complex. A. Schematic representation of the multi-step purification protocol employed to isolate the TolC-YbjP and TolC-YbjP-AcrABZ complexes. **B.** Cryo-EM processing workflow. **C.** Local resolution distribution in final map[54]. **D.** Gold-standard Fourier Shell Correlation curves for final reconstruction[55]. **E.** Angular distribution plot for final map.

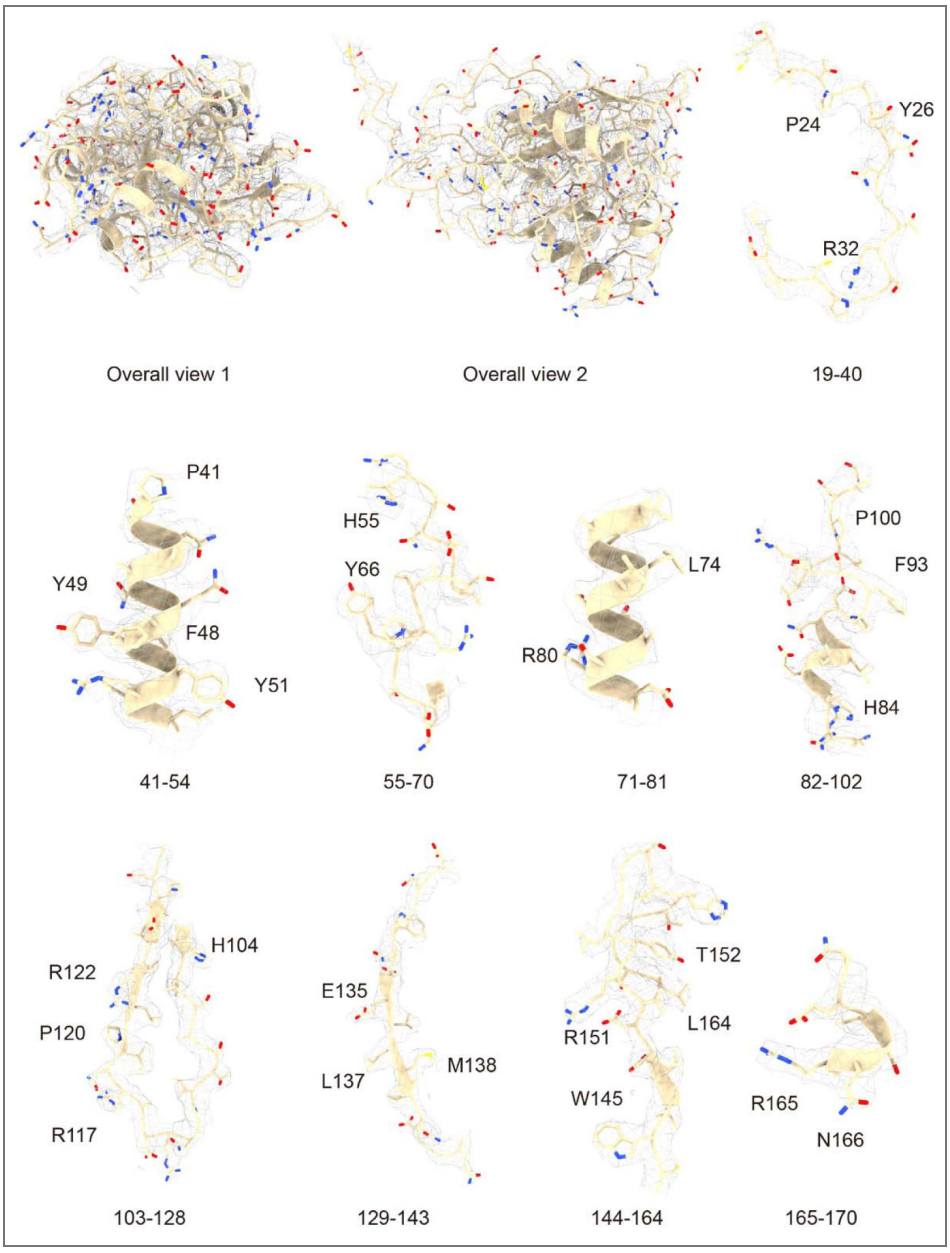

Figure S2. Local EM-density of YbjP in TolC-YbjP complex.

The region and some bulky residues are labelled. EM density threshold: 8σ.

Figure S3. Structural comparison of the anchoring domains from six prototypical efflux pump outer membrane factors.

Cartoon representations of the protomer structures from *E. coli* TolC-YbjP (PDB: 9V52; this study), *K. pneumoniae* TOprJ1 (AlphaFold model/PDB: 9J3D)[56], *C. jejuni* CmeC (PDB: 4MT4)[57], *E. coli* CusC (PDB: 3PIK)[19,58], *P. aeruginosa* OprM (PDB: 3D5K)[18], and *V. cholera* VceC (AlphaFold model/PDB: 1YC9)[59] are shown. The conserved structural region responsible for anchoring the pump to the outer membrane is highlighted within the dashed box for each structure.

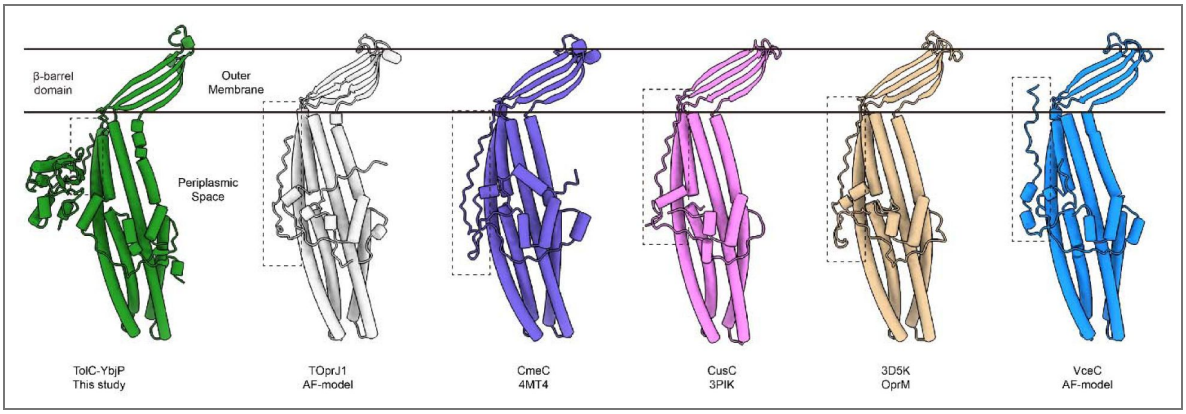

Figure S4. Cryo-EM processing workflow for TolC-YbjP-AcrABZ complex.

A. Cryo-EM processing workflow. **B.** Local resolution distribution in C1 final map[54]. **C.** Gold-standard Fourier Shell Correlation curves for C1 final reconstruction[55]. **D.** Angular distribution plot for C1 final map. **E.** Local resolution distribution in C3 final map[54]. **F.** Gold-standard Fourier Shell Correlation curves for C3 final reconstruction[55]. **G.** Angular distribution plot for C3 final map.

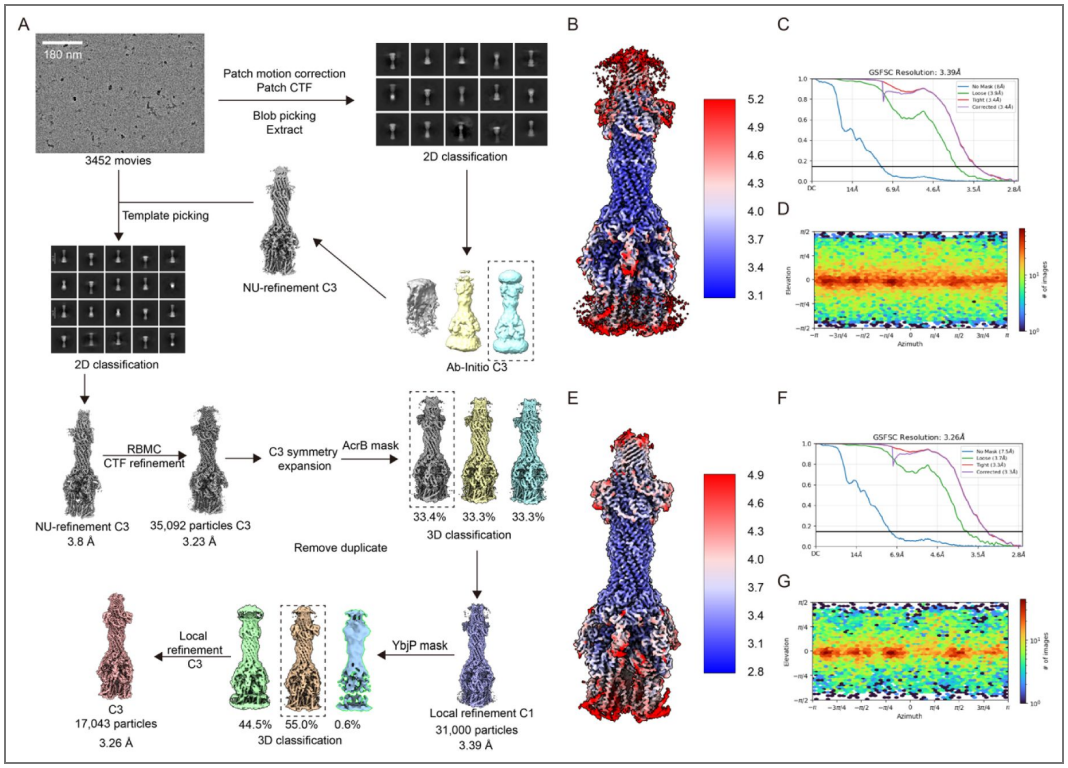

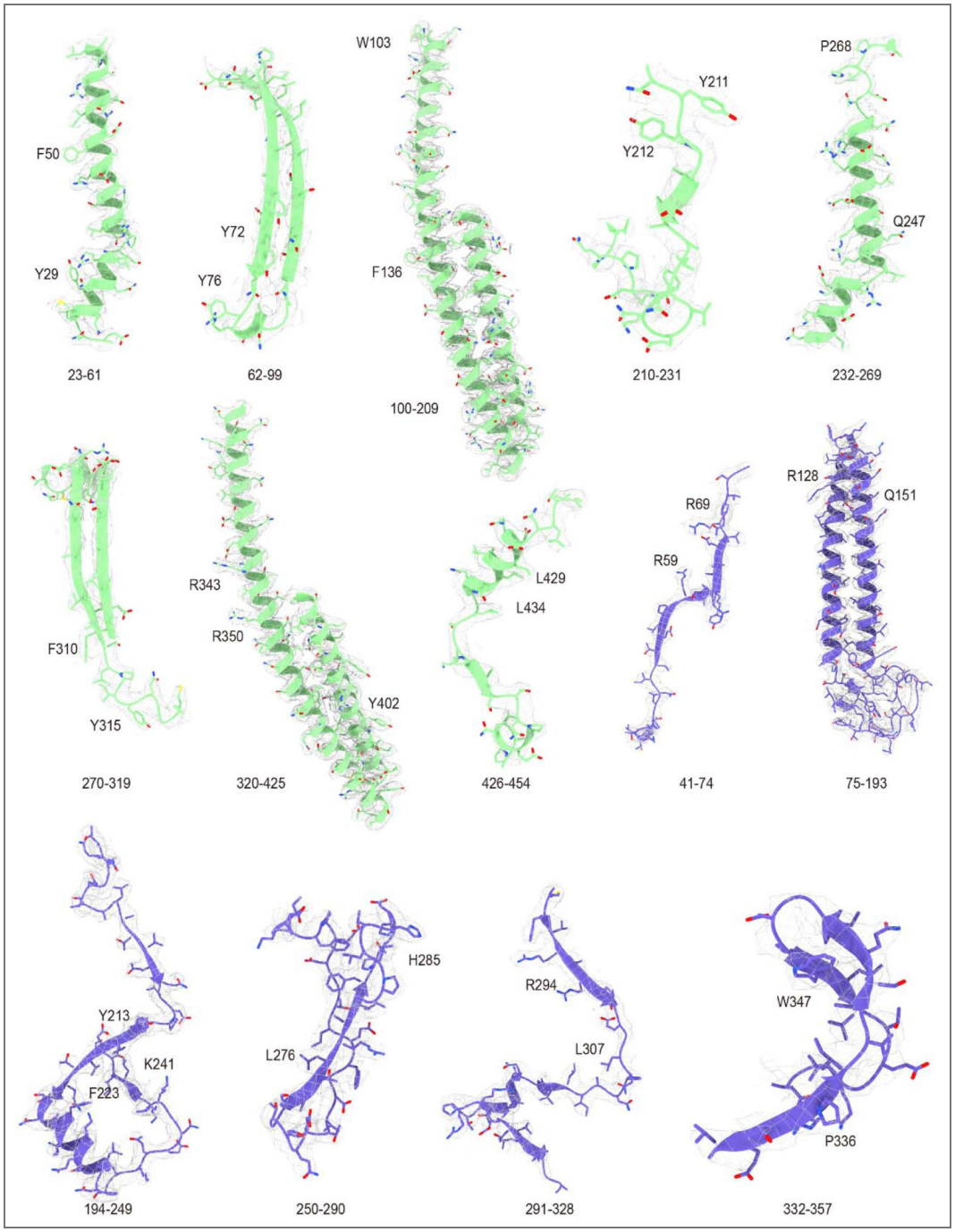

Figure S5. Local EM-density of TolC and AcrA in TolC-YbjP-AcrABZ complex.

The region and some bulky residues are labelled. EM density threshold: 8σ.

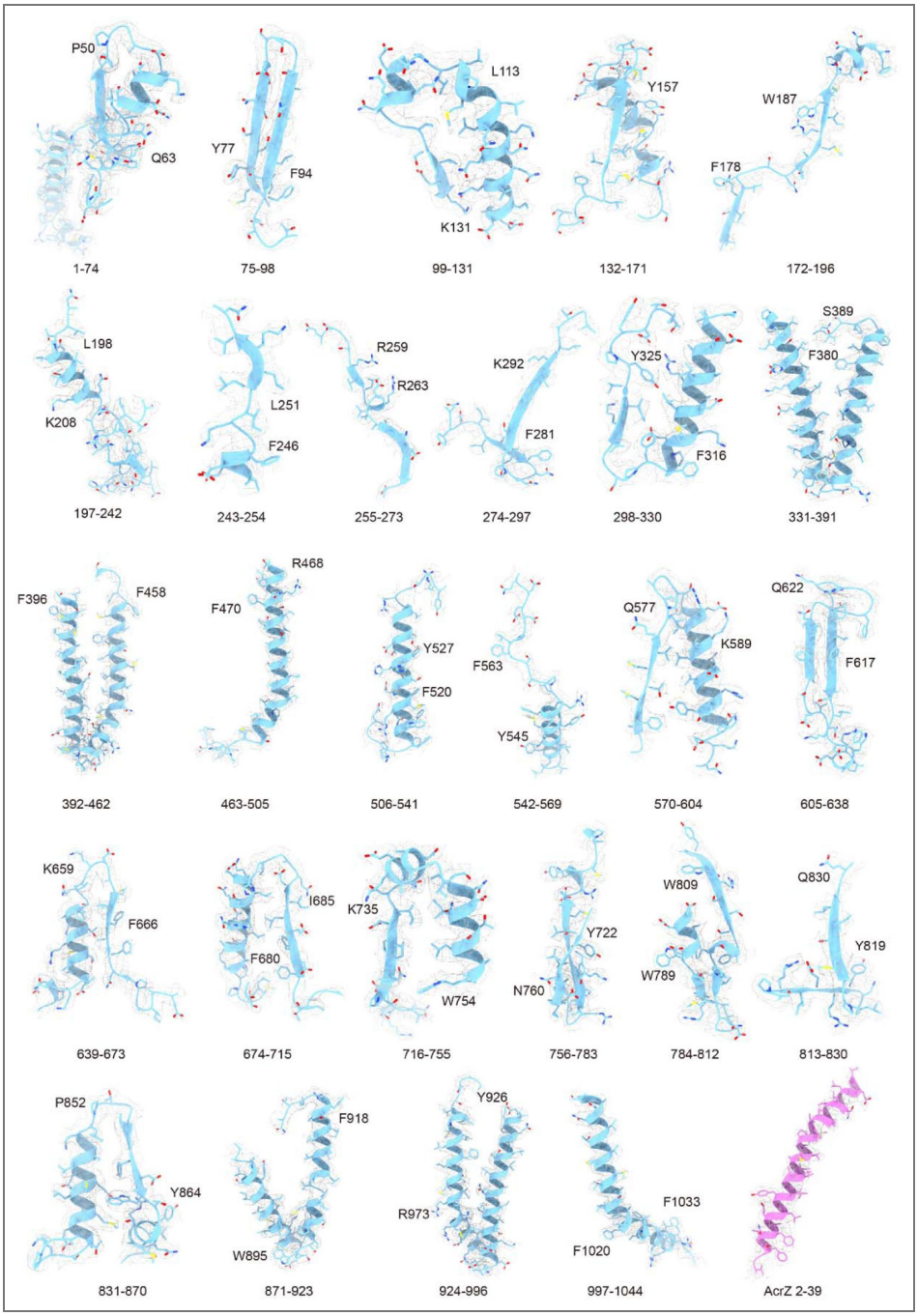

Figure S6. Local EM-density of AcrB and AcrZ in TolC-YbjP-AcrABZ complex.

The region and some bulky residues are labelled. EM density threshold: 5σ.

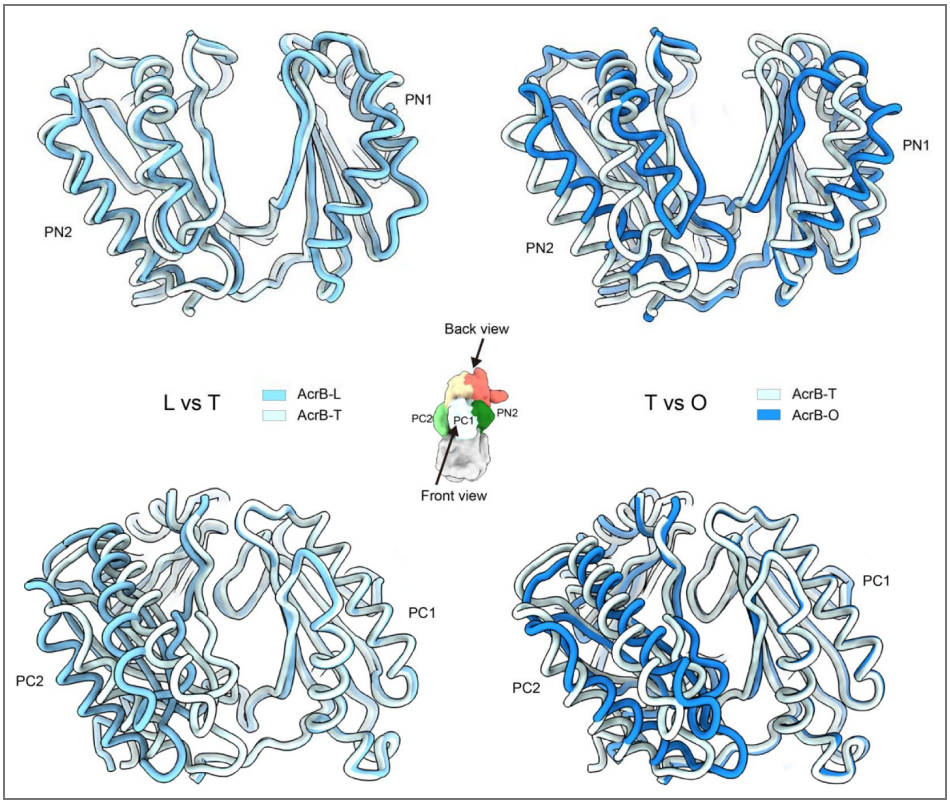

Figure S7. Conformational transitions in AcrB's porter domain during the transport cycle.

Structural superposition of porter domain (subdomains PN1, PN2, PC1 and PC2) of monomers between L and T states and T and O states, revealing key conformational rearrangements.

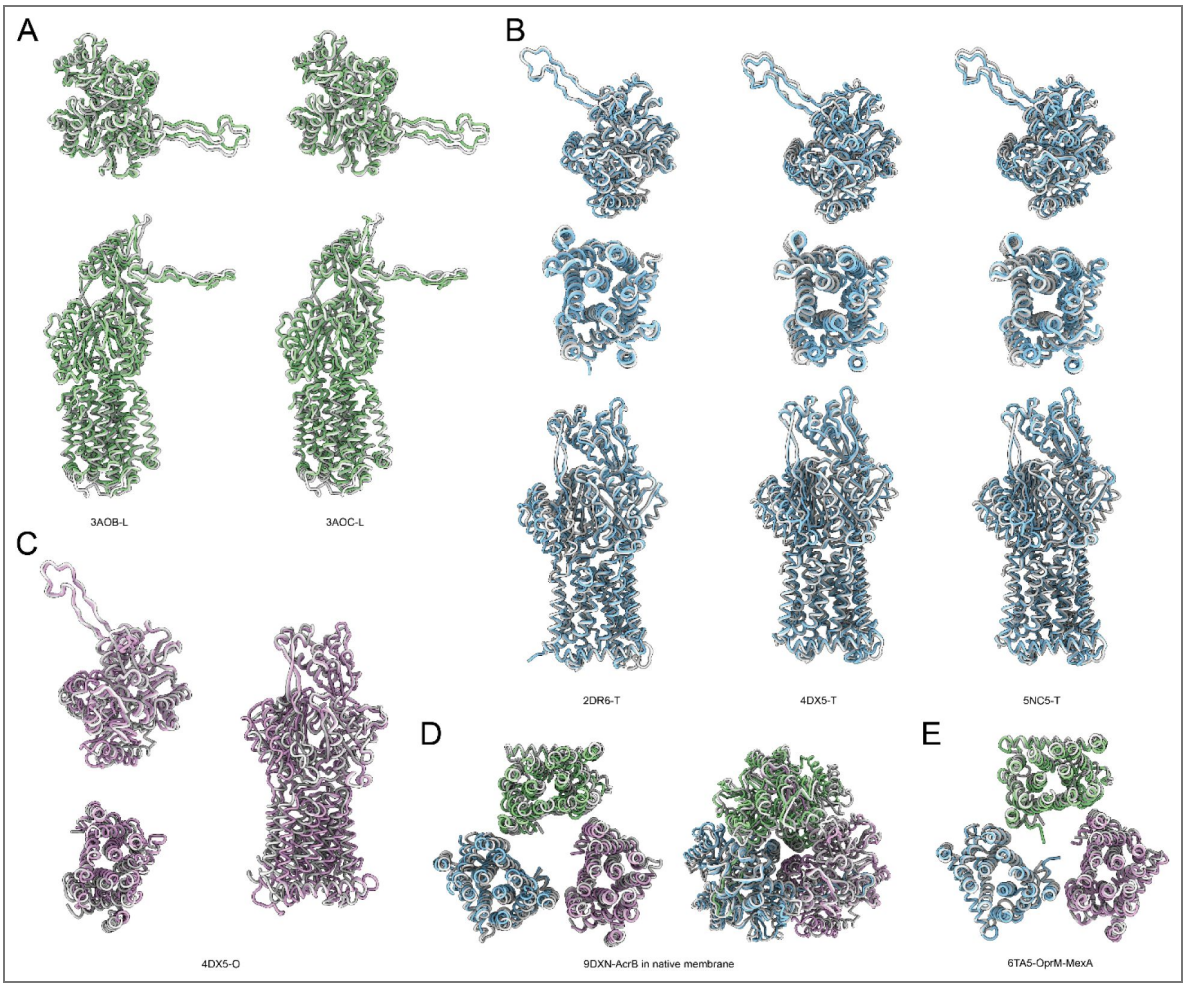

Figure S8. Structural comparison of AcrB conformational states.

A. Comparison of the AcrB L state from the holocomplex with known L-state structures (PDB: 3AOB, 3AOC)[60]. Top panels show the funnel and porter domains (top view); bottom panels show a single protomer (side view). **B.** Comparison of the AcrB T state with reference T-state structures (PDB: 2DR6, 4DX5, 5NC5)[17,20,31]. Panels show top views of the funnel and porter domains (top) and transmembrane domains (middle), and a side view of a protomer (bottom). **C.** Detailed comparison of the AcrB O state with 4DX5[20], using the same three views as in (B). **D.** Comparison of the AcrB structure from the holocomplex with an AcrB structure determined in the native membrane environment (PDB: 9DXN). **E.** Comparison of the AcrB transmembrane domain with that of the homologous MexB (PDB: 6TA5)[30].

Supplementary Tables

	TolC-YbjP	TolC-YbjP-AcrABZ	TolC-YbjP-AcrA (local)
Voltage (kV)	300		
Electron exposure ($e^-/Å^2$)	50		
Defocus range (μm)	-1.2 ~ -1.8		
Pixel size (Å)	1.35		
Micrographs (no.)	3452		
Symmetry imposed	C3	C1	C3
Final particle images (no.)	63,022	31,000	17,043
Map resolution (Å) 0.143 FSC threshold	3.56	3.39	3.26
Map sharpening B factor ($Å^2$)	-134.5	-66.6	-74.7
CC (model vs. data)	0.7945	0.8727	0.8456
Model composition			
Chain count	6	18	12
Non-hydrogen atoms	13,539	53,464	29,061
Protein residues	1,752	7,037	3,816
B factors ($Å^2$)			
Proteins	40.66	99.69	115.5
R.m.s. deviations			
Bond lengths (Å)	0.006	0.003	0.006
Bond angles (°)	0.665	0.498	0.697
Validation			
MolProbity score	2.05	1.63	1.77
Clashscore	11.62	7.22	7.94
Poor rotamers (%)	0.41	0.12	0.13
Ramachandran plot			
Favored (%)	92.47	96.49	95.15
Allowed (%)	7.36	3.36	4.56
Disallowed (%)	0.17	0.16	0.29
PDB code	9V52	9V53	9V55
EMDB code	EMD-64784	EMD-64785	EMD-64787

Table S1. **Cryo-EM data collection, refinement and validation statistics**

Data availability

Cryo-EM maps and the associated structural coordinates have been respectively deposited into the Electron Microscopy Data Bank (EMDB) and the Protein Data Bank (PDB) under the following accession codes: EMD-64784 / 9V52 (TolC-YbjP); EMD-64785 / 9V53 (TolC-YbjP-AcrABZ); and EMD-64787 / 9V55 (TolC-YbjP-AcrA local).

Acknowledgements

We are thankful to the Tsinghua University Branch of the China National Center for Protein Sciences (Beijing) for their generous assistance with cryo-EM facility support and computational resources on the Bio-Computing Platform cluster. Additionally, we appreciate the valuable technical support from J. Lei, X. Li, and F. Yang. This work was supported by the Science and Technology Development Fund, Macau SAR (FDCT) (Grant No. 0112/2025/ITP2 to X.G.), the National Natural Science Foundation of China (Grant Nos. 32501078 to X.G., and 32371254 to J.W.), and the Natural Science Foundation of Beijing Municipality (Grant No. 5262009 to J.W.).

Additional information

Author contributions

X.G. and J.W. conceived the project. X.G. and Z.G. optimized the preparation of cryo-grids, recorded the cryo-EM data, and processed this data. J.W. built the atomic models. X.G. and J.W. wrote the manuscript. All authors read and approved the final version of the manuscript.

Funding

Funder	Grant reference number	Author
MOST | National Natural Science Foundation of China (NSFC)	32501078	Xiaofei Ge
MOST | National Natural Science Foundation of China (NSFC)	32371254	Jiawei Wang
北京市科学技术委员会 | Natural Science Foundation of Beijing Municipality (北京市自然科学基金)	5262009	Jiawei Wang
Science and Technology Development Fund, Macau SAR (FDCT)	0112/2025/ITP2	Xiaofei Ge

Author ORCID iDs

Xiaofei Ge: https://orcid.org/0009-0005-9626-7061
Jiawei Wang: https://orcid.org/0000-0001-9893-8539

References

1 **Poole K.** (2005) Efflux-mediated antimicrobial resistance. *J Antimicrob Chemother* **56**:20-51 https://doi.org/10.1093/jac/dki171 | PubMed

2 **Li X. Z.,** Plésiat P., Nikaido H (2015) The challenge of efflux-mediated antibiotic resistance in Gram-negative bacteria. *Clin Microbiol Rev* **28**:337-418 https://doi.org/10.1128/cmr.00117-14 | PubMed

3 **Du D.,** van Veen H. W., Murakami S., Pos K. M., Luisi B. F (2015) Structure, mechanism and cooperation of bacterial multidrug transporters. *Curr Opin Struct Biol* **33**:76-91 https://doi.org/10.1016/j.sbi.2015.07.015 | PubMed

4 **Du D. J.,** et al. (2018) Multidrug efflux pumps: structure, function and regulation. *Nature Reviews Microbiology* **16**:523-539 https://doi.org/10.1038/s41579-018-0048-6 | PubMed

5 **Blair J. M.,** Richmond G. E., Piddock L. J (2014) Multidrug efflux pumps in Gram-negative bacteria and their role in antibiotic resistance. *Future Microbiol* **9**:1165-1177 https://doi.org/10.2217/fmb.14.66 | PubMed

6 **Wright M.,** Kaur M., Thompson L. K., Cox G (2025) A historical perspective on the multifunctional outer membrane channel protein TolC in Escherichia coli. *NPJ Antimicrob Resist* **3**:6 https://doi.org/10.1038/s44259-025-00078-3 | PubMed

7 **Ma D.,** et al. (1995) Genes acrA and acrB encode a stress-induced efflux system of Escherichia coli. *Mol Microbiol* **16**:45-55 https://doi.org/10.1111/j.1365-2958.1995.tb02390.x | PubMed

8 **Nikaido H** (2009) Multidrug resistance in bacteria. *Annu Rev Biochem* **78**:119-146 https://doi.org/10.1146/annurev.biochem.78.082907.145923 | PubMed

9 **Okusu H.,** Ma D., Nikaido H (1996) AcrAB efflux pump plays a major role in the antibiotic resistance phenotype of Escherichia coli multiple-antibiotic-resistance (Mar) mutants. *J Bacteriol* **178**:306-308 https://doi.org/10.1128/jb.178.1.306-308.1996 | PubMed

10 **Koronakis V.,** Sharff A., Koronakis E., Luisi B., Hughes C (2000) Crystal structure of the bacterial membrane protein TolC central to multidrug efflux and protein export. *Nature* **405**:914-919 https://doi.org/10.1038/35016007 | PubMed

11 **Mikolosko J.,** Bobyk K., Zgurskaya H. I., Ghosh P (2006) Conformational flexibility in the multidrug efflux system protein AcrA. *Structure* **14**:577-587 https://doi.org/10.1016/j.str.2005.11.015 | PubMed

12 **Murakami S.,** Nakashima R., Yamashita E., Yamaguchi A (2002) Crystal structure of bacterial multidrug efflux transporter AcrB. *Nature* **419**:587-593 https://doi.org/10.1038/nature01050 | PubMed

13 **Shi X.,** et al. (2019) In situ structure and assembly of the multidrug efflux pump AcrAB-TolC. *Nat Commun* **10**:2635 https://doi.org/10.1038/s41467-019-10512-6 | PubMed

14 **Pei X. Y.,** et al. (2011) Structures of sequential open states in a symmetrical opening transition of the TolC exit duct. *Proc Natl Acad Sci U S A* **108**:2112-2117 https://doi.org/10.1073/pnas.1012588108 | PubMed

15 **Andersen C.,** et al. (2002) Transition to the open state of the ToIC periplasmic tunnel entrance. *Proceedings of the National Academy of Sciences of the United States of America* **99**:11103-11108 https://doi.org/10.1073/pnas.162039399 | PubMed

16 **Bavro V. N.,** et al. (2008) Assembly and channel opening in a bacterial drug efflux machine. *Mol Cell* **30**:114-121 https://doi.org/10.1016/j.molcel.2008.02.015 | PubMed

17 **Wang Z.,** et al. (2017) An allosteric transport mechanism for the AcrAB-TolC multidrug efflux pump. *eLife* **6** https://doi.org/10.7554/eLife.24905 | PubMed

18 **Phan G.,** et al. (2010) Structural and dynamical insights into the opening mechanism of P. aeruginosa OprM channel. *Structure* **18**:507-517 https://doi.org/10.1016/j.str.2010.01.018 | PubMed

19 **Kulathila R.,** Kulathila R., Indic M., van den Berg B. (2011) Crystal structure of Escherichia coli CusC, the outer membrane component of a heavy metal efflux pump. *PLoS One* **6**:e15610 https://doi.org/10.1371/journal.pone.0015610 | PubMed

20 **Eicher T.,** et al. (2012) Transport of drugs by the multidrug transporter AcrB involves an access and a deep binding pocket that are separated by a switch-loop. *Proc Natl Acad Sci U S A* **109**:5687-5692 https://doi.org/10.1073/pnas.1114944109 | PubMed

21 **Holm L.,** Laiho A., Törönen P., Salgado M (2023) DALI shines a light on remote homologs: One hundred discoveries. *Protein Sci* **32**:e4519 https://doi.org/10.1002/pro.4519 | PubMed

22 **Dong C.,** et al. (2013) Structural insights into the inhibition of type VI effector Tae3 by its immunity protein Tai3. *Biochem J* **454**:59-68 https://doi.org/10.1042/bj20130193 | PubMed

23 **Varadi M.,** et al. (2022) AlphaFold Protein Structure Database: massively expanding the structural coverage of protein-sequence space with high-accuracy models. *Nucleic Acids Res* **50**:D439-d444 https://doi.org/10.1093/nar/gkab1061 | PubMed

24 **Xu K.,** et al. (2019) A^2-net: molecular structure estimation from cryo-EM density volumes. In: 33rd AAAI Conference on Artificial Intelligence / 31st Innovative Applications of Artificial Intelligence Conference / 9th AAAI Symposium on Educational Advances in Artificial Intelligence. pp. 1230-1237

25 **Horne J.,** et al. (2025) A lipoprotein partner for the Escherichia coli outer membrane protein TolC. *bioRxiv* https://doi.org/10.1101/2025.03.19.644130

26 **Du D.,** et al. (2020) Interactions of a Bacterial RND Transporter with a Transmembrane Small Protein in a Lipid Environment. *Structure* **28**:625-634.e626 https://doi.org/10.1016/j.str.2020.03.013 | PubMed

27 **Alav I.,** et al. (2021) Structure, Assembly, and Function of Tripartite Efflux and Type 1 Secretion Systems in Gram-Negative Bacteria. *Chem Rev* **121**:5479-5596 https://doi.org/10.1021/acs.chemrev.1c00055 | PubMed

28 **Andersen C.,** Koronakis E., Hughes C., Koronakis V (2002) An aspartate ring at the TolC tunnel entrance determines ion selectivity and presents a target for blocking by large cations. *Mol Microbiol* **44**:1131-1139 https://doi.org/10.1046/j.1365-2958.2002.02898.x | PubMed

29 **Marshall R. L.,** Bavro V. N (2020) Mutations in the TolC Periplasmic Domain Affect Substrate Specificity of the AcrAB-TolC Pump. *Front Mol Biosci* **7**:166 https://doi.org/10.3389/fmolb.2020.00166 | PubMed

30 **Glavier M.,** et al. (2020) Antibiotic export by MexB multidrug efflux transporter is allosterically controlled by a MexA-OprM chaperone-like complex. *Nat Commun* **11**:4948 https://doi.org/10.1038/s41467-020-18770-5 | PubMed

31 **Murakami S.,** Nakashima R., Yamashita E., Matsumoto T., Yamaguchi A (2006) Crystal structures of a multidrug transporter reveal a functionally rotating mechanism. *Nature* **443**:173-179 https://doi.org/10.1038/nature05076 | PubMed

32 **Seeger M. A.,** et al. (2006) Structural asymmetry of AcrB trimer suggests a peristaltic pump mechanism. *Science* **313**:1295-1298 https://doi.org/10.1126/science.1131542 | PubMed

33 **Delmar J. A.,** Su C. C., Yu E. W. (2014) Bacterial multidrug efflux transporters. *Annual Review of Biophysics* **43**:93-117 https://doi.org/10.1146/annurev-biophys-051013-022855 | PubMed

34 **Yu Z.,** Shi X., Wang Z. (2024) Structures and Efflux Mechanisms of the AcrAB-TolC Pump. In: Robin Harris J., Marles-Wright Jon (Eds). *Macromolecular Protein Complexes V: Structure and Function* Springer International Publishing. pp. 1-16

35 **Boyer P. D** (1997) The ATP synthase - A splendid molecular machine. *Annual Review of Biochemistry* **66**:717-749 https://doi.org/10.1146/annurev.biochem.66.1.717 | PubMed

36 **Lazarova M.,** et al. (2025) Conformational plasticity across phylogenetic clusters of RND multidrug efflux pumps and its impact on substrate specificity. *Nat Commun* **16**:11649 https://doi.org/10.1038/s41467-025-66751-3 | PubMed

37 **Liu H.,** Tse C. M., Dang S (2025) Capturing the native structure of membrane proteins using vesicles. *Proc Natl Acad Sci U S A* **122**:e2423407122 https://doi.org/10.1073/pnas.2423407122 | PubMed

38 **Zgurskaya H. I.,** Nikaido H (2000) Cross-linked complex between oligomeric periplasmic lipoprotein AcrA and the inner-membrane-associated multidrug efflux pump AcrB from Escherichia coli. *Journal of Bacteriology* **182**:4264-4267 https://doi.org/10.1128/jb.182.15.4264-4267.2000 | PubMed

39 **Touzé T.,** et al. (2004) Interactions underlying assembly of the Escherichia coli AcrAB-TolC multidrug efflux system. *Molecular Microbiology* **53**:697-706 https://doi.org/10.1111/j.1365-2958.2004.04158.x | PubMed

40 **Szal T.,** et al. (2025) Disassembly of the Escherichia coli AcrABZ-TolC efflux pump by ligand-mediated disruption of TolC-AcrA interfacial contacts. *bioRxiv* https://doi.org/10.1101/2025.02.18.638599

41 **Zwama M.,** et al. (2018) Multiple entry pathways within the efflux transporter AcrB contribute to multidrug recognition. *Nature Communications* **9** https://doi.org/10.1038/s41467-017-02493-1 | PubMed

42 **Smith B. L.,** Fernando S., King M. D. (2024) Escherichia coli resistance mechanism AcrAB-TolC efflux pump interactions with commonly used antibiotics: a molecular dynamics study. Scientific Reports. https://doi.org/10.1038/s41598-024-52536-z | PubMed

43 **Su C. C.,** et al. (2006) Conformation of the AcrB multidrug efflux pump in mutants of the putative proton relay pathway. *Journal of Bacteriology* **188**:7290-7296 https://doi.org/10.1128/jb.00684-06 | PubMed

44 **Yue Z.,** Chen W., Zgurskaya H. I., Shen J. N (2017) Constant pH Molecular Dynamics Reveals How Proton Release Drives the Conformational Transition of a Transmembrane Efflux Pump. *Journal of Chemical Theory and Computation* **13**:6405-6414 https://doi.org/10.1021/acs.jctc.7b00874 | PubMed

45 **Lei J.,** Frank J (2005) Automated acquisition of cryo-electron micrographs for single particle reconstruction on an FEI Tecnai electron microscope. *Journal of structural biology* **150**:69-80 https://doi.org/10.1016/j.jsb.2005.01.002 | PubMed

46 **Punjani A.,** Rubinstein J. L., Fleet D. J., Brubaker M. A (2017) cryoSPARC: algorithms for rapid unsupervised cryo-EM structure determination. *Nat Methods* **14**:290-296 https://doi.org/10.1038/nmeth.4169 | PubMed

47 **Pettersen E. F.,** et al. (2004) UCSF Chimera--a visualization system for exploratory research and analysis. *J Comput Chem* **25**:1605-1612 https://doi.org/10.1002/jcc.20084 | PubMed

48 **Emsley P.,** Lohkamp B., Scott W. G., Cowtan K. (2010) Features and development of Coot. *Acta Crystallogr D Biol Crystallogr* **66**:486-501 https://doi.org/10.1107/S0907444910007493 | PubMed

49 **Afonine P. V.,** et al. (2018) Real-space refinement in PHENIX for cryo-EM and crystallography. *Acta Crystallogr D Struct Biol* **74**:531-544 https://doi.org/10.1107/S2059798318006551 | PubMed

50 **Brown A.,** et al. (2015) Tools for macromolecular model building and refinement into electron cryo-microscopy reconstructions. *Acta Crystallogr D Biol Crystallogr* **71**:136-153 https://doi.org/10.1107/s1399004714021683 | PubMed

51 **DeLano W. L** (2002) The PyMOL Molecular Graphics System. *on World Wide Web* http://www.pymol.org

52 **Meng E. C.,** et al. (2023) UCSF ChimeraX: Tools for structure building and analysis. *Protein Sci* **32**:e4792 https://doi.org/10.1002/pro.4792 | PubMed

53 **Smart O. S.,** Neduvelil J. G., Wang X., Wallace B. A., Sansom M. S (1996) HOLE: a program for the analysis of the pore dimensions of ion channel structural models. *J Mol Graph* **14**:354-360 https://doi.org/10.1016/s0263-7855(97)00009-x | PubMed

54 **Kucukelbir A.,** Sigworth F. J., Tagare H. D (2014) Quantifying the local resolution of cryo-EM density maps. *Nat Methods* **11**:63-65 https://doi.org/10.1038/nmeth.2727 | PubMed

55 **Rosenthal P. B.,** Henderson R (2003) Optimal determination of particle orientation, absolute hand, and contrast loss in single-particle electron cryomicroscopy. *J Mol Biol* **333**:721-745 https://doi.org/10.1016/j.jmb.2003.07.013 | PubMed

56 **Shi Y.,** et al. (2025) Assembly and inhibition of transferable TMexCD1-TOprJ1 efflux pump. *Nat Commun* **16**:10025 https://doi.org/10.1038/s41467-025-65038-x | PubMed

57 **Su C. C.,** et al. (2014) Crystal structure of the Campylobacter jejuni CmeC outer membrane channel. *Protein Sci* **23**:954-961 https://doi.org/10.1002/pro.2478 | PubMed

58 **Su C. C.,** et al. (2011) Crystal structure of the CusBA heavy-metal efflux complex of Escherichia coli. *Nature* **470**:558-562 https://doi.org/10.1038/nature09743 | PubMed

59 **Federici L.,** et al. (2005) The crystal structure of the outer membrane protein VceC from the bacterial pathogen Vibrio cholerae at 1.8 A resolution. *J Biol Chem* **280**:15307-15314 https://doi.org/10.1074/jbc.M500401200 | PubMed

60 **Nakashima R.,** Sakurai K., Yamasaki S., Nishino K., Yamaguchi A (2011) Structures of the multidrug exporter AcrB reveal a proximal multisite drug-binding pocket. *Nature* **480**:565-U199 https://doi.org/10.1038/nature10641 | PubMed

Peer reviews

Reviewer #1 (Public review):

Summary:

This manuscript investigates the biological mechanism underlying the assembly and transport of the AcrAB-TolC efflux pump complex. By combining endogenous protein purification with cryo-EM analysis, the authors show that the AcrB trimer adopts three distinct conformations simultaneously and identify a previously uncharacterized lipoprotein, YbjP, as a potential additional component of the complex. The work aims to advance our understanding of the AcrAB-TolC efflux system in near-native conditions and may have broader implications for elucidating its physiological mechanism.

Strengths:

Overall, the manuscript is clearly presented, and several of the datasets are of high quality. The use of natively isolated complex is a major strength, as it minimizes artifacts associated with reconstituted systems and enables the discovery of a novel subunit. The authors also distinguish two major assemblies-the TolC-YbjP sub-complex and the complete pump-which appear to correspond to the closed and open channel states, respectively. The conceptual advance is potentially meaningful, and the findings could be of broad interest to the field.

Weaknesses:

(1) As the identification of YbjP is a key contribution of this work, a deeper comparison with functional "anchor" proteins in other efflux pumps is needed. Including an additional supplementary figure illustrating these structural comparisons would be valuable.

(2) The observation of the LTO states in the presence of TolC represents an important extension of previous findings. A more detailed discussion comparing these LTO states to those reported in earlier structural and biochemical studies would improve the clarity and significance of this point.

Comments on revisions:

In the revision, the authors have addressed the above concerns to improve this study.

https://doi.org/10.7554/eLife.109684.2.sa2

Reviewer #2 (Public review):

Summary:

This manuscript reports the high-resolution cryo-EM structures of the endogenous TolC-YbjP-AcrABZ complex and a TolC-YbjP subcomplex from E. coli, identifying a novel accessory subunit. This work is an impressive effort that provides valuable structural insights into this native complex.

Strengths:

(1) The study successfully determines the structure of the complete, endogenously purified complex, marking a significant achievement.

(2) The identification of a previously unknown accessory subunit is an important finding.

(3) The use of cryo-EM to resolve the complex, including potential post-translational modifications such as N-palmitoyl and S-diacylglycerol, is a notable highlight.

Weaknesses:

(1) Clarity and Interpretation: Several points need clarification. Additionally, the description of the sample preparation method, which is a key strength, is currently misplaced and should be introduced earlier.

(2) Data Presentation: The manuscript would benefit significantly from improved figures.

(3) Supporting Evidence: The inclusion of the protein purification profile as a supplementary figure is essential. Furthermore, a discussion comparing the endogenous AcrB structure to those obtained in other systems (e.g., liposomes) and commenting on observed lipid densities would strengthen the overall analysis.

Comments on revisions:

In the revision, all my concerns have been addressed.

https://doi.org/10.7554/eLife.109684.2.sa1

Author Response:

The following is the authors' response to the original reviews.

> ***Public Reviews:***
>
> ***Reviewer #1 (Public review):***
>
> *Summary:*
>
> *This manuscript investigates the biological mechanism underlying the assembly and transport of the AcrAB-TolC efflux pump complex. By combining endogenous protein purification with cryo-EM analysis, the authors show that the AcrB trimer adopts three distinct conformations simultaneously and identify a previously uncharacterized lipoprotein, YbjP, as a potential additional component of the complex. The work aims to advance our understanding of the AcrAB-TolC efflux system in near-native conditions and may have broader implications for elucidating its physiological mechanism.*
>
> *Strengths:*
>
> *Overall, the manuscript is clearly presented, and several of the datasets are of high quality. The use of natively isolated complexes is a major strength, as it minimizes artifacts associated with reconstituted systems and enables the discovery of a novel subunit. The authors also distinguish two major assemblies-the TolC-YbjP sub-complex and the complete pump-which appear to correspond to the closed and open channel states, respectively. The conceptual advance is potentially meaningful, and the findings could be of broad interest to the field.*
>
> *Weaknesses:*
>
> *(1) As the identification of YbjP is a key contribution of this work, a deeper comparison with functional "anchor" proteins in other efflux pumps is needed. Including an additional Supplementary Figure illustrating these structural comparisons would be valuable.*

We have expanded the comparative analysis between YbjP and established anchoring or accessory components in other efflux pumps, and we have added Supplementary Figure S3 to

illustrate these structural relationships.

> *(2) The observation of the LTO states in the presence of TolC represents an important extension of previous findings. A more detailed discussion comparing these LTO states to those reported in earlier structural and biochemical studies would improve the clarity and significance of this point.*

In the revised manuscript we have expanded our discussion of the LTO conformations, including a direct comparison with previously reported structural and biochemical observations, to better contextualize the significance of our findings.

> ***Reviewer #2 (Public review):***
>
> *Summary:*
>
> *This manuscript reports the high-resolution cryo-EM structures of the endogenous TolC-YbjP-AcrABZ complex and a TolC-YbjP subcomplex from E. coli, identifying a novel accessory subunit. This work is an impressive effort that provides valuable structural insights into this native complex.*
>
> *Strengths:*
>
> *(1) The study successfully determines the structure of the complete, endogenously purified complex, marking a significant achievement.*
>
> *(2) The identification of a previously unknown accessory subunit is an important finding.*
>
> *(3) The use of cryo-EM to resolve the complex, including potential post-translational modifications such as N-palmitoyl and S-diacylglycerol, is a notable highlight.*
>
> *Weaknesses:*
>
> *(1) Clarity and Interpretation: Several points need clarification. Additionally, the description of the sample preparation method, which is a key strength, is currently misplaced and should be introduced earlier.*

We have reorganized the text to introduce the sample preparation strategy earlier and clarify the points that may cause ambiguity.

> *(2) Data Presentation: The manuscript would benefit significantly from improved figures.*

We agree and have revised the figures to improve clarity, consistency, and readability. Additional schematic illustrations have been included.

> *(3) Supporting Evidence: The inclusion of the protein purification profile as a supplementary figure is essential. Furthermore, a discussion comparing the endogenous AcrB structure to those obtained in other systems (e.g., liposomes) and commenting on observed lipid densities would strengthen the overall analysis.*

We appreciate these suggestions. We added the purification profile to Supplementary Figure S1 and expanded the comparison between our endogenous AcrB structure and previously reported structures from reconstituted systems, including a more detailed discussion of lipid densities.

> ***Reviewer #3 (Public review):***
>
> *Summary:*
>
> *The manuscript "Structural mechanisms of pump assembly and drug transport in the AcrAB-TolC efflux system" by Ge et al. describes the identification of a previously*

> *uncharacterized lipoprotein, YbjP, as a novel partner of the well-studied Enterobacterial tripartite efflux pump AcrAB-TolC. The authors present cryo-electron microscopy structures of the TolC-YbjP subcomplex and the complete AcrABZ-TolC-YbjP assembly. While the identification and structural characterization of YbjP are potentially novel, the stated focus of the manuscript-mechanisms of pump assembly and drug transport - is not sufficiently addressed. The manuscript requires reframing to emphasize the principal novelty associated with YbjP and significant development of the other aspects, especially the claimed novelty of the AcrB drug-efflux cycle.*
>
> *Strengths:*
>
> *The reported association of YbjP with AcrAB-TolC is novel; however, a recent deposition of a preceding and much more detailed manuscript to the BioRxiv server (Horne et al., https://doi.org/10.1101/2025.03.19.644130) removes much of the immediate novelty.*
>
> *Weaknesses:*
>
> *While the identification of YbjP is novel, the authors do not appear to acknowledge the precedence of another work (Horne et al., 2025), and it is not cited within the correct context in the manuscript.*

We thank the reviewer for raising this important point regarding the independent nature of our work.

Our study indeed progressed independently. The process began with our purification of an endogenous protein sample containing the AcrAB-TolC efflux pump. During our cryo-EM analysis, we observed an unassigned density in the map, for which we built a preliminary main-chain model. A subsequent search of structural databases, including AlphaFold predictions, allowed us to identify this density as the protein YbjP. It was only after this identification that we became aware of the related preprint by Horne et al. on BioRxiv (Posted March 19, 2025).

Therefore, our structural determination of YbjP was conducted entirely independently. We fully acknowledge and respect the work by Horne et al. and have already cited their preprint in our manuscript. While their detailed structural data, maps, and coordinates were not publicly available as of March 13, 2026, we have described their findings appropriately. We agree that our manuscript can better reflect this context and will carefully check for any missing citations to ensure that their contribution is properly and clearly acknowledged.

We also believe that the two studies are mutually complementary and collectively reinforce the emerging understanding of YbjP.

> *Several results presented in the TolC-YbjP section do not represent new findings regarding TolC structure itself.*

We agree that the TolC features we describe are consistent with previously reported structural characteristics. However, these observations could only be confirmed in the context of the newly determined TolC–YbjP subcomplex, which was not available prior to this study. We have clarified this point in the revision to avoid overstating novelty.

> *The structure and gating behaviour of TolC should be more thoroughly introduced in the Introduction, including prior work describing channel opening and conformational transitions.*

We appreciate this suggestion and agree that a more comprehensive overview of TolC gating and conformational transitions will strengthen the Introduction. We have revised the text to incorporate relevant prior structural and functional studies.

> *The current manuscript does not discuss the mechanistic role of helices H3/H4 and H7/H8 in channel dilation, despite implying that YbjP binding may influence these features.*

Thank you for this comment. The primary novel contributions of this manuscript are the identification of YbjP and the structural characterization of AcrB in three distinct states. The discussion of the dilation mechanism, while included because we observed the closed TolC-YbjP state, is a secondary point. In the revised manuscript, we have expanded this discussion as suggested.

> *Only the original closed TolC structure is cited, and the manuscript does not address prior mutational studies involving the D396 region, though this residue is specifically highlighted in the presented structures.*

We appreciate the reviewer drawing attention to this oversight. We have added citations to the relevant mutational and mechanistic studies, including those involving the D396 region, and more clearly discussed these findings in relation to our structural observations.

> *The manuscript provides only a general structural alignment between the closed TolC-YbjP subcomplex and the open TolC observed in the full pump assembly. However, multiple open, closed, and intermediate conformations of AcrAB-TolC have already been reported. Thus, YbjP alone cannot be assumed to account for TolC channel gating. A systematic comparison with existing structures is necessary to determine whether YbjP contributes any distinct allosteric modulation.*

We agree with the reviewer's assessment and appreciate the constructive suggestion. In our revised manuscript, we have expanded the structural comparison to include previously reported open, closed, and intermediate AcrAB–TolC conformations. This expanded analysis will more clearly position our findings within the existing structural framework.

> *The analysis of AcrB peristaltic action is superficial, poorly substantiated and importantly, not novel. Several references to the ATP-synthase cycle have been provided, but this has been widely established already some 20 years ago - e.g. https://www.science.org/doi/10.1126/science.1131542.*

We thank the reviewer for this comment. We fully acknowledge the foundational studies that established the AcrB functional cycle and its analogy to the ATP-synthase mechanism. While previous work indeed defined the LTO (Loose, Tight, Open) cycle of AcrB, those structures were obtained using AcrB in isolation. In contrast, our endogenous sample, which includes the native constraints of AcrA from above and the presence of AcrZ, reveals conformational changes in the transmembrane and porter domains that differ from those previously reported. We interpret these differences as reflecting a more physiologically relevant mechanism. In our revision, we provided a detailed discussion to contextualize these distinctions within the existing literature.

> *The most significant limitation of the study is the absence of functional characterization of YbjP in vivo or in vitro. While the structural association between YbjP and TolC is interesting, the biological role of YbjP remains unclear.*

To explore the potential physiological role of YbjP, we compared the viability of a *ΔybjP* mutant in the *E. coli C600* background with that of the wild-type C600 strain under ciprofloxacin (CIP) stress. However, we did not observe a detectable difference in survival between the two strains under the tested conditions. This result is consistent with the assay reported in the preprint mentioned by the reviewer, although the stress conditions used in that study differ from ours.

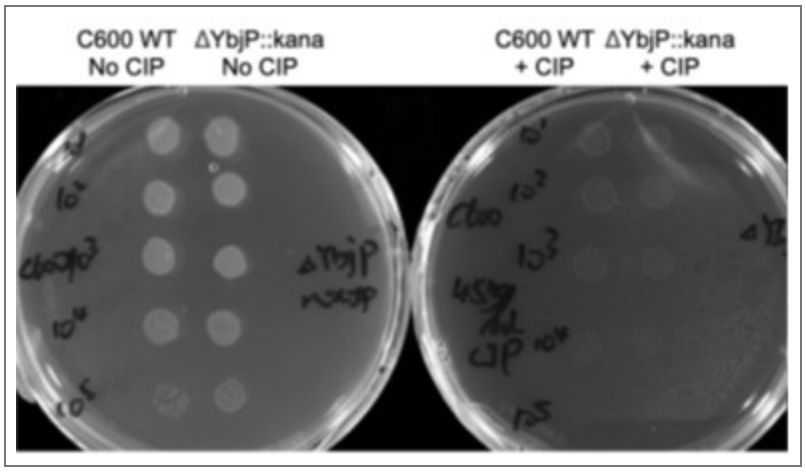

Author response image 1.

To further address this point, we have added a new Supplementary Figure S3 comparing outer membrane proteins with structural and functional similarities to TolC. As shown in this analysis, many such proteins contain an extracellular loop that appears to help anchor or stabilize them within the outer membrane. Notably, TolC lacks such a loop, whereas YbjP contains a corresponding loop region, suggesting that YbjP may potentially play a role in stabilizing or positioning TolC in the outer membrane.

While our current experiments did not reveal a clear phenotype under CIP stress, the structural observations still suggest that YbjP may have a physiological role. We have therefore expanded the Discussion to more carefully consider possible functional implications of YbjP and to explicitly acknowledge the limitations of the present study regarding its physiological characterization.

> *Moreover, the manuscript does not examine structural differences between the presented complex and previously solved AcrAB-TolC or MexAB-OprM assemblies that might support a mechanistic model.*

We thank the reviewer for this suggestion. We now provide a more detailed comparative analysis with previously reported AcrAB–TolC and MexAB–OprM structures, highlighting both similarities and key differences.

Recommendations for the authors:

> ***Reviewer #1 (Recommendations for the authors):***
>
> *(1) To address the probable role of YbjP, performing 3D variability analysis on the sub-complex and the complete complex would help clarify whether YbjP participates in channel opening and closing.*

YbjP does not participate in the opening or closing of the TolC channel. Indeed, the structure of TolC shows no conformational changes upon YbjP binding when compared to the free, closed form of TolC. The structural transition between the closed and open states of TolC has been thoroughly reviewed by Alav et al. (Chem. Rev. 2021).

Although the particles for the two reconstructions were obtained from the same dataset, inspection of the raw micrographs and the corresponding 2D class averages clearly shows that the particles fall into two distinct populations: one containing only the TolC–YbjP sub-complex and the other containing the full AcrABZ–TolC–YbjP assembly. In other words, the particles correspond to two different complexes, distinguished by the absence or presence of

the AcrABZ components, rather than representing two conformational states of a single complex.

Three-dimensional variability analysis (3DVA) is most appropriate for analyzing structural heterogeneity arising from continuous or discrete conformational changes within the same macromolecular assembly. Because the heterogeneity in our dataset primarily reflects compositional differences between two assemblies rather than conformational variability within a single complex, we believe that applying 3DVA would not be appropriate for this dataset.

> *(2) In addition to the above points, a few minor revisions would improve clarity and readability. Some of the representative density maps in the supplementary figures could be refined for clarity. Adjusting formatting elements (e.g., dashed line thickness) may improve visual presentation.*

Supplementary Figures S2, S5, and S6 have been redrawn to reduce the excessive thickness of the density map representations for better visualization.

> ***Reviewer #2 (Recommendations for the authors):***
>
> *In this manuscript, Xiaofei and colleagues report the high-resolution cryo-EM structure of the TolC-YbjP-AcrABZ complex, as well as the structure of a subcomplex containing only TolC and YbjP. Additionally, they identify a previously unidentified accessory subunit that plays a role in the function of this complex. Overall, this represents an impressive effort in determining the complete endogenous complex from E. coli and performing systematic analyses. I have a few questions regarding the manuscript:*
>
> *(1) The authors use the term "native" several times (e.g., lines 24, 73, 157, 256) to refer to the complex reported here. This may cause confusion, given the use of detergent to extract endogenous complexes from E. coli. They should consider excluding the possibility that the subcomplex was formed during the purification process. The term "endogenous" should suffice in this context.*

We have replaced “native” with “endogenous”.

> *(2) Lines 26-28: The phrase "its protomers" may lead to ambiguity, as it could refer to either YbjP or TolC.*

The sentence has been updated to “…bridging the TolC protomers at their equatorial domain.”

> *(3) Lines 50-51: The text suggests that the assembly of AcrA and AcrB triggers TolC's transition from a closed to an open conformation. Please clarify this point.*

The introduction (lines 50-51) has been expanded to describe the assembly of TolC and AcrAB, as well as the gating transition between the closed and open states of TolC.

> *(4) Lines 57-59: Using cryo-EM may get the low-to-medium resolution map, but not using low-to-medium resolution cryo-EM.*

The sentence has been changed to … prior studies using crystallography and cryo-EM have revealed low-to-medium resolution snapshots of the assembled pump.

> *(5) Line 73: The authors should consider briefly introducing how they prepared the samples for cryo-EM structural studies, as this is a highlight of the manuscript.*

A detailed, multi-step purification protocol has been added as Supplementary Figure S1A to illustrate the sample preparation procedure.

> *(6) Lines 77-82: The authors should label these structural features in the corresponding figures for easier reference, particularly clarifying which part refers to the "equatorial domain."*

We have labeled these structural features in the corresponding figures for clarity, and specifically indicated which region corresponds to the equatorial domain.

> *(7) Lines 92-93: The first α-helix of TolC is unclear; the authors should indicate the corresponding residues of this helix in the main text. Additionally, it would be beneficial to illustrate the interface in a figure for easier access.*

We have specified the residues corresponding to the participating α-helix of TolC in the main text and illustrated the interaction interface in a figure (Figure 1F) for better visualization.

> *(8) Lines 99-100: Did the authors observe additional density for N-palmitoyl and S-diacylglycerol modifications in their cryo-EM density map? If so, they should highlight this in a figure to demonstrate the importance of these modifications.*

The N-palmitoyl and S-diacylglycerol modifications are embedded in the outer membrane but lack a consistent location within it. As a result, they were averaged out during cryo-EM reconstruction and are not visible in our final map.

> *(9) Line 122: Please indicate the 33 nm height in the figure.*

The 33 nm height is composed of a 14 nm TolC channel, a 14 nm periplasmic portion of AcrAB, and a 5 nm transmembrane portion of AcrB, which has been added to the right side of Figure 2B.

> *(10) Lines 123-124: This sentence feels out of place. It would be more appropriate to move it to another location, such as the beginning of the Results section, to introduce how the samples were prepared.*

This sentence has been moved to the section “Structure of a TolC–YbjP closed-state complex” to describe the sample preparation.

> *(11) Lines 127-128: This section needs to be rewritten for improved clarity.*

This sentence has been rewritten as “This tripartite architecture is stabilized by three distinct sets of interfaces: (i) contacts between the AcrB trimer and the basal regions of AcrA, (ii) extensive AcrA–AcrA lateral interactions within the hexameric ring, and (iii) tip-to-tip junctions formed between the upper AcrA α-helical hairpin and the periplasmic entrance of TolC (Figure 2D).”

> *(12) Line 141: Please define terms like DN, DC, PN, and PC upon their first use.*

DN and DC (denoting the N- and C-terminal subdomains of the docking domain), PN and PC (named for the N- and C-terminal subdomains of the periplasmic (porter) domain) have been defined where they first appear in the text.

> *(13) The lα helix of AcrB is at least partially buried in the membrane (Liu H. et al, PNAS 2025). The authors should consider including this information in their figures, particularly Figure 2B and Figure 5. As the complex is endogenously purified, are there any differences in AcrB compared to those observed in liposomes, SMALP, or vesicles? Did the authors observe significant lipid densities?*

A structural comparison of the AcrB holocomplex with an AcrB structure determined in the native membrane environment (PDB: 9DXN) has been added as Supplementary Figure S8D.

In the transmembrane region of AcrB, some sausage-like densities were observed; however, lipid molecules were not modelled in the study.

> *(14) The protein purification profile should be included, at least as a supplementary figure.*

The protein purification profile has been added to Supplementary Figure S1A.

> ***Reviewer #3 (Recommendations for the authors):***
>
> *(1) The identification and structural characterization of YbjP as a novel TolC-associated lipoprotein is potentially interesting, and the cryo-EM structures of the TolC-YbjP subcomplex and the complete pump assembly represent a solid starting point. However, the manuscript currently does not sufficiently support the broader mechanistic conclusions implied by the title regarding pump assembly and drug transport. To strengthen the work, the manuscript would benefit from being refocused to highlight the novelty of YbjP, while also providing a clearer mechanistic rationale for its functional role.*

We thank the reviewer for this helpful comment. We have revised the manuscript to better highlight the novel features of YbjP and provide a clearer mechanistic explanation for its function.

Most Gram-negative TolC homologs, including *P. aeruginosa* OprM and *E. coli* CusC, carry native lipid anchors that attach them to the outer membrane. However, *E. coli* TolC lacks this N-terminal lipidation site. We propose that YbjP, a dually lipidated protein modified with N-palmitoyl and S-diacylglycerol groups, tethers TolC to the outer membrane and functionally replaces the intrinsic lipid anchors found in other outer membrane factors.

To support this mechanism, we have added Supplementary Figure S3, which compares the anchoring domains of six representative outer membrane components of efflux pumps.

> *(2) The structural features and gating dynamics of TolC should be more thoroughly introduced, including prior work describing channel dilation and helix movements (e.g., PMID: 18406332; PMID: 21245342), and the manuscript should discuss how YbjP may influence these known conformational transitions. The relevance of the D396 region should also be considered in the context of previous mutational analyses (e.g., PMID: 32850959).*

All citations mentioned have been added. Indeed, the structure of TolC shows no conformational changes upon YbjP binding when compared to the free, closed form of TolC.

> *(3) Structural interpretation of the YbjP-containing complexes needs to be strengthened by comparison with the extensive library of available AcrAB-TolC structures in open, closed, and intermediate states (e.g., PMID: 28355133; PMID: 24747401; PMID: 34506732). Such analysis is necessary to determine whether YbjP contributes any distinct allosteric or conformational effects.*

YbjP binds to the equatorial domain of TolC, distant from the tip of its coiled-coil helices. This binding therefore does not interfere with TolC's functional role, but rather helps anchor TolC within the outer membrane in the correct orientation.

> *(4) The speculations regarding the peristaltic nature of AcrB cycling as currently presented in the text and Figure 4 lack novelty and currently reiterate well-established AcrB L/T/O states without offering insight into how YbjP might influence long-range communication within the complex.*

We thank the reviewer for this valuable comment. We agree that the functional rotation mechanism of AcrB with loose, tight and open states has been well documented in previous work.

In our endogenous intact complex, however, we identified substantial conformational changes in both the porter and transmembrane domains of AcrB that were not observed in earlier isolated structures. To highlight these differences, we have added Supplementary Figure S8 to compare our AcrB structure with all previously reported conformational states.

On the basis of these structural observations, we have proposed a distinct drug efflux mechanism, which is now described in detail in the revised manuscript.

> *(5) Specific clarification is needed regarding the proposed pathway by which YbjP could modulate AcrA or AcrB, given the spatial separation observed in the structures.*

YbjP binds to the equatorial domain of TolC, which has no effect on AcrA or AcrB.

> *(6) The manuscript currently lacks functional validation of YbjP, either in vivo or in vitro. Incorporating even basic assays to test YbjP's contribution to efflux function, pump assembly, or antibiotic resistance would significantly enhance the conclusions.*

To explore the potential physiological role of YbjP, we compared the viability of a *ΔybjP* mutant in the *E. coli C600* background with that of the wild-type C600 strain under ciprofloxacin (CIP) stress. However, we did not observe a detectable difference in survival between the two strains under the tested conditions. This result is consistent with the assay reported in the preprint mentioned by the reviewer, although the stress conditions used in that study differ from ours. (See Author response image 1).

To further address this point, we have added a new Supplementary Figure (Fig. S3) comparing outer membrane proteins with structural and functional similarities to TolC. As shown in this analysis, many such proteins contain an extracellular N-terminal loop that appears to help anchor or stabilize them within the outer membrane. Notably, TolC lacks such a loop, whereas YbjP contains a corresponding loop region, suggesting that YbjP may potentially play a role in stabilizing or positioning TolC in the outer membrane.

While our current experiments did not reveal a clear phenotype under CIP stress, the structural observations still suggest that YbjP may have a physiological role. We have therefore expanded the Discussion to more carefully consider possible functional implications of YbjP and to explicitly acknowledge the limitations of the present study regarding its physiological characterization.

> *(7) The relationship to the prior BioRxiv work by Horne et al. (March 19, 2025) should be discussed more directly, particularly because it reports the same YbjP-TolC association across two different efflux systems and includes higher-resolution structures and functional evidence. The current citation should be revised to accurately acknowledge the precedence and overlap in findings.*

We thank the reviewer for this important suggestion. We have adjusted the citation to earlier in the manuscript to properly acknowledge the work by Horne et al.

We fully agree that a direct comparison between our structures and those reported by Horne et al. would be highly valuable. However, although nearly a year has passed since the preprint was posted, their atomic coordinates have not been released in the Protein Data Bank. No detailed structural coordinates or models are provided in the preprint itself, which prevents us from performing a meaningful, structure-based comparison with our own data at this stage.

> *(8) The references used to support statements on allosteric pump activation (e.g., lines 182-183) should be updated to include more relevant full-complex studies (e.g., PMID: 28355133; PMID: 33009415; PMID: 33909410), and the manuscript should more clearly articulate any proposed mechanism for signal transmission involving YbjP.*

The citations have been added.

YbjP does not participate in the opening or closing of the TolC channel. Indeed, the structure of TolC shows no conformational changes upon YbjP binding when compared to the free, closed form of TolC.

> *(9) Overall, while the structural identification of YbjP is noteworthy, additional functional data and more rigorous structural comparison are needed to substantiate the proposed model of pump assembly and drug transport. Reframing the manuscript to emphasize the novelty of YbjP and clarifying its potential mechanistic role would strengthen the work significantly.*

We refer the reviewer to our earlier response for additional functional data. We have added Supplementary Figure S8 to compare our AcrB structure with all previously reported conformational states.

https://doi.org/10.7554/eLife.109684.2.sa0